



## From soil to cave: Transport of trace metals by natural organic matter in karst dripwaters

Adam Hartland <sup>a,b,c,\*</sup>, Ian J. Fairchild <sup>a</sup>, Jamie R. Lead <sup>a</sup>, Andrea Borsato <sup>d</sup>, Andy Baker <sup>b,c</sup>, Silvia Frisia <sup>e</sup>, Mohammed Baalousha <sup>a</sup>

<sup>a</sup> School of Geography, Earth and Environmental Sciences, College of Life and Environmental Sciences, University of Birmingham, Edgbaston, Birmingham, B15 2TT, UK

<sup>b</sup> Connected Waters Initiative Research Centre, Water Research Laboratory, University of New South Wales, 110 King St, Manly Vale, NSW, 2093 Australia

<sup>c</sup> Affiliated to the National Centre for Groundwater Research and Training, Australia

<sup>d</sup> Museo delle Scienze, Via Calepina 14, 38122 Trento, Italy

<sup>e</sup> School of Environmental and Life Sciences, University of Newcastle, Callaghan 2308 NSW, Australia

### ARTICLE INFO

#### Article history:

Received 6 May 2011

Received in revised form 21 January 2012

Accepted 25 January 2012

Available online 8 February 2012

#### Keywords:

Colloids  
Nanoparticles  
Soil organic matter  
Complexation  
Hydrology  
Speleothems

### ABSTRACT

This paper aims to establish evidence for the widespread existence of metal binding and transport by natural organic matter (NOM) in karst dripwaters, the imprint of which in speleothems may have important climatic significance. We studied the concentration of trace metals and organic carbon (OC) in sequentially filtered dripwaters and soil leachates from three contrasting sites: Poole's Cavern (Derbyshire, UK), Lower Balls Green Mine (Gloucestershire, UK) and Grotta di Ernesto (Trentino, Italy). The size-distribution of metals in the three soils was highly similar, but distinct from that found in fractionated dripwaters: surface-reactive metals were concentrated in the coarse fraction ( $> 100$  nm) of soils, but in the fine colloidal ( $< 100$  nm) and nominally dissolved ( $< 1$  nm) fractions of dripwaters. The concentration of Cu, Ni and Co in dripwater samples across all sites were well correlated ( $R^2 = 0.84$  and  $0.70$ , Cu vs. Ni, Cu vs. Co, respectively), indicating a common association. Furthermore, metal ratios (Cu:Ni, Cu:Co) were consistent with NICA-Donnan  $n_1$  humic binding affinity ratios for these metals, consistent with a competitive hierarchy of binding affinity (Cu  $>$  Ni  $>$  Co) for sites in colloidal or dissolved NOM. Large shifts in Cu:Ni in dripwaters coincided with high fluxes of particulate OC (following peak infiltration) and showed increased similarity to ratios in soils, diagnostic of qualitative changes in NOM supply (i.e. fresh inputs of more aromatic/hydrophobic soil organic matter (SOM) with Cu outcompeting Ni for suitable binding sites). Results indicate that at high-flows (i.e. where fracture-fed flow dominates) particulates and colloids migrate at similar rates, whereas, in slow seepage-flow dripwaters, particulates ( $> 1$   $\mu$ m) and small colloids (1–100 nm) decouple, resulting in two distinct modes of NOM–metal transport: high-flux and low-flux. At the hyperalkaline drip site PE1 (in Poole's Cavern), high-fluxes of metals (Cu, Ni, Zn, Ti, Mn, Fe) and particulate NOM occurred in rapid, short-lived pulses following peak infiltration events, whereas low-fluxes of metals (Co and V  $>$  Cu, Ni and Ti) and fluorescent NOM ( $<$  ca. 100 nm) were offset from infiltration events, probably because small organic colloids (1–100 nm) and solutes ( $<$  1 nm) were slower to migrate through the porous matrix than particulates. These results demonstrate the widespread occurrence of both colloidal and particulate NOM–metal transport in cave dripwaters and the importance of karst hydrology in affecting the breakthrough times of different species. Constraints imposed by soil processes (colloid/particle release), direct contributions of metals and NOM from rainfall, and flow-routing (colloid/particle migration) are expected to determine the strength of correlations between NOM-transported metals in speleothems and climatic signals. Changes in trace metal ratios (e.g. Cu:Ni) in speleothems may encode information on NOM composition, potentially aiding in targeting of compound-specific investigations and for the assessment of changes in the quality of soil organic matter.

Crown Copyright © 2012 Published by Elsevier B.V. All rights reserved.

### 1. Introduction

It is widely recognised that natural organic matter (NOM) plays a dominant role as a complexing agent for trace metals in natural systems (i.e. surface waters, groundwaters and soils). The term “natural organic matter” encompasses all the organic matter (OM) in a given reservoir excluding living organisms and anthropogenic compounds (Filella, 2008). Despite the diverse array of biopolymers present

\* Corresponding author at: Connected Waters Initiative Research Centre, Water Research Laboratory, University of New South Wales, 110 King St, Manly Vale, NSW, 2093 Australia. Tel.: +61 2 8071 9800.

E-mail address: [a.hartland@unsw.edu.au](mailto:a.hartland@unsw.edu.au) (A. Hartland).

(Kelleher and Simpson, 2006), the majority of studies have focused on the extracted humic fraction of NOM, largely because humic substances (HS) are readily separated and are considered to be the chemically most significant NOM fraction (Tipping, 2001).

The term 'humic substances', or the description of compounds as having 'humic-like' character are used here in a functional sense only (e.g. for cation binding). The evolving view of HS should be emphasised: that HS do not represent a unique compound class but instead are mixtures of predominantly low-molecular weight components probably stabilised through hydrophobic interactions and hydrogen bonding (Sutton and Sposito, 2005; Aitken et al., 2011), although this understanding is still limited by differences between analytical methods which give contrasting answers (Lead and Wilkinson, 2006; Filella, 2008).

In this paper, we seek to understand the hydrogeochemical role of aqueous NOM in trace metal binding and transport in speleothem-forming dripwaters. The "NOM" term is used here generically to encompass the particulate (solids with a dimension  $> 1 \mu\text{m}$ ), colloidal (solids with a dimension between 1 nm and  $1 \mu\text{m}$ ), and dissolved organic matter (DOM;  $< 1 \text{ nm}$ ) in cave waters, unless otherwise specified.

In natural waters, aqueous particulates, colloids, and DOM compete to bind trace metals (Nimmo and Fones, 1997; Warnken et al., 2007; Pedrot et al., 2008). Particulates may be more readily removed from percolating solutions by pore blockage, permitting colloids and DOM to dominate the transport of complexed (i.e. chemically bound) cationic species (McCarthy and McKay, 2004). This process is well known from field and column studies, but there have been few published studies of naturally occurring, trace element transport by these agents in karstic groundwaters (McCarthy and Shevenell, 1998; Mavrocordatos et al., 2000), and only recently has this process been identified in cave percolation waters that feed speleothems (calcareous cave precipitates) (Hartland et al., 2011). The process has however, been modelled extensively in relation to groundwater systems (Bekhit et al., 2009) and used to explain enhanced transport of metals (Chen et al., 2005; Hartland et al., 2010a), radionuclides (Kersting et al., 1999) and pollutants in general (White et al., 2005).

Transport of trace elements by NOM in karst systems is of specific interest to studies of the elemental composition of speleothems (Fairchild et al., 2006a; Fairchild and Treble, 2009), and has been identified as a potentially important vector for a suite of surface-reactive metals (Hartland et al., 2011). This process may become manifest in speleothems as annual, to sub-annual, synchronous variations in organic fluorescence and trace metals (e.g. Cu, Ni, Zn, Pb, Y, REE<sup>3+</sup>) (Roberts et al., 1998; Huang et al., 2001; Richter et al., 2004; Borsato et al., 2007; Zhou et al., 2008), and where strong seasonal variations in effective rainfall occur, NOM-transported trace elements in speleothems may be quantitatively linked to rainfall amount (Jo et al., 2010), with a component potentially originating in the rainwater itself (Nimmo and Fones, 1997; Witt and Jickells, 2005; Gilfedder et al., 2007; Muller et al., 2008) as well as overlying soils.

Temporal studies have shown that pronounced increases in NOM concentration and fluorescence occur in cave waters during hydrologically active periods in northern temperate (Baker et al., 1997, 1999a,b; Fairchild et al., 2006b), sub-tropical (Cruz et al., 2005) and monsoonal climates (Tan et al., 2006; Ban et al., 2008). However, the transmission of fluorescent NOM in percolation waters is often temporally offset from rainfall maxima. Possible mechanisms for this delay include decoupling of the soil–aquifer system as a result of soil-moisture deficit (Baker et al., 1997, 2000; Cruz et al., 2005), aquifer drying (Baker et al., 2000), and differential hydrological routing between drips (Tooth and Fairchild, 2003). However, the breakthrough times of particulate, colloidal, and dissolved NOM in dripwaters have not been examined and because coarse colloids ( $> 100 \text{ nm}$ ) and particulates ( $> 1 \mu\text{m}$ ) may be less prone to matrix diffusion (diffusion into micropores and fractures) than fine colloids (1–100 nm) and solutes ( $< 1 \text{ nm}$ ), they may be transmitted more quickly (McCarthy and McKay, 2004).

Variations in NOM have the potential to be usefully applied as a tracer of groundwater hydrology and UV-fluorescence has been used in numerous studies (Baker et al., 1997; Baker and Genty, 1999; Tan et al., 2006). However, NOM fluorescence is susceptible to disruption by inner-filtering (i.e. self-absorption, Hudson et al., 2007) and, where present, the coarse fraction masks fluorescence in finer fractions (Hartland et al., 2010b). Fluorescence attributes of NOM may also be quantitatively related to its functional properties (Baker et al., 2008). For example, humic-like (Peak C) fluorescence emission wavelengths in the typical range of cave waters (ca. 400–420 nm) correlate with weaker metal binding, whereas longer Peak C emission wavelengths, characteristic of more aromatic/hydrophobic NOM, correlate with stronger binding (Baker et al., 2008). But whether this relates to conformational or compositional changes in the NOM as yet remains unproven (Hartland et al., 2010b).

Detailed spatial and temporal studies of the interaction between NOM and trace metals in cave waters are needed to better understand the processes behind the incorporation of NOM (Blyth et al., 2008) and associated inorganic constituents of speleothems (Borsato et al., 2007; Fairchild and Treble, 2009). Ultimately, we must also address the influence of biotic and abiotic changes to the NOM during its transmission and the importance of drip hydrochemistry for these processes (Einsiedl et al., 2007).

This paper provides a first analysis of NOM and trace metal partitioning between size classes in sequentially filtered soil leachates and cave dripwaters to assess the potential for soil-derived trace elements and NOM to reach speleothems and provide a signal of infiltration. Wet and dry deposition also contribute organic matter and trace metals to soils, and the concentrations of these constituents in rainwaters often occupy a similar range to that found in karst waters (Nimmo and Fones, 1997; Muller et al., 2008), and therefore we have included data from a rainfall monitoring station near the main study site for comparison. Variations in the intensity of fluorescence, total organic carbon (TOC) and trace element contents of sequentially filtered karst dripwater samples from three contrasting sites are presented and compared to leached soil samples. In essence, this work seeks to identify the particulate, colloidal and dissolved components in dripwaters that are responsible for trace element transport, examine how these differ from soils, whether these differ significantly between sites, and whether differences with time reflect hydrology.

The distinction between aqueous phases (e.g. colloidal vs. dissolved) is often blurred and is largely method dependant (Lead and Wilkinson, 2006). Throughout the text we refer to size classes derived from sequential membrane filtrations, although this size-based differentiation can allow retention of materials smaller than the nominal pore size cut off and passage of larger material such that the accuracy of the separation of size fractions is not absolute.

## 2. Study sites

Three contrasting study sites were targeted in this study: Poole's Cavern (PC), Buxton, UK; Lower Balls Green Mine (LBGM), Minchinhampton, UK; and Grotta di Ernesto (ERN), Trentino, NE Italian Alps (Fig. S1–4). The rationale in selecting these sites was to assess the importance of differences in soils and karst hydrology on NOM–metal transport: PC and ERN have organic-rich soils and are forested; PC is dominated by matrix-flow, whereas ERN is fracture dominated; and finally LBGM has slowly permeable, clay-rich soils and a mixture of seepage- and fracture-fed flow regimes. Hydrologic and hydrogeochemical information on the drip points studied is summarised in Table 1 and their average geochemistry is given in Table S1. The soil physical characteristics are described in Table 2 and the chemistry of the soil leachates is given Table 3.

Drip rates of PC dripwaters (PE1 and BC1) and LBGM drips (LB1–3) were monitored at 30 second intervals using Driptych Stalagmate-Plus™ (Egham, UK) drip rate loggers from June 2008 to

**Table 1**  
Summary dripwater hydrology, indicative hydrochemical properties and drip point characteristics.

Site	RSD of discharge (%)	Max discharge ( $\mu\text{L s}^{-1}$ )	Mean discharge ( $\mu\text{L s}^{-1}$ )	Drip classification <sup>a</sup>	pH	Electro conductivity ( $\mu\text{S cm}^{-1}$ )	High Mg/Ca or Sr/Ca at low flow? (PCP)	Drip point type	Speleothem morphology (modern precipitate) at impact point
<i>Poole's Cavern</i>									
BC1	27	87	58.4	Seepage flow	7.91 ± 0.22	496 ± 42.1	No/no	Crack in ceiling	Active flowstone
BC2	32	42	27.7	Seepage flow	7.88 ± 0.17	501 ± 41.7	No/no	Crack in ceiling	Active flowstone
PE1 <sup>b</sup>	75	49	8.7	Seasonal (fast)	11.50 ± 0.73	703 ± 257	No/no	Short soda straw	Incipient cone-shaped stalagmite
RC1	149	35	5.4	Seasonal (slow)	11.77 ± 1.46	1878 ± 1413	No/no	Long soda straw	Cone-shaped stalagmite
RC2	114	95	27.8	Seasonal (fast)	12.71 ± 0.10	1946 ± 1547	No/no	Short soda straw	Incipient candle-shaped stalagmite
<i>Lower Balls Green Quarry</i>									
LB1	58	501	195	Vadose flow	8.07 ± 0.14	520 ± 11.1	??/?	Crack in ceiling	Active flowstone
LB2	20	539	401	Percolation stream	8.08 ± 0.12	498 ± 94.4	??/?	Crack in ceiling	Active flowstone
LB3	76	366	27.3	Vadose flow	8.12 ± 0.07	521 ± 31.7	??/?	Short soda straw	Active flowstone/incipient stalagmite
<i>Grotta d'Ernesto</i>									
St-1 <sup>c</sup>	88	390	207	Seasonal (fast)	7.87 ± 0.05	284 ± 3.9	Yes/no (minor)	Stalactite	Active flowstone
St-2 <sup>d</sup>	78	600	41.7	Seasonal (fast)	7.86 ± 0.07	282 ± 10.5	Yes/yes (minor)	Short soda straw	Cone-shaped stalagmite
St-ER77	32	3.1	2.4	Seepage flow	8.04 ± 0.13	287 ± 0.8	??/?	Soda straw	Cone-shaped stalagmite
St-ER78	115	1.1	0.5	Seasonal (slow)	7.81 ± 0.05	281 ± 0.1	??/?	Thick stalactite pendant	Incipient cone-shaped stalagmite

St = stalactite; designation of Grotta d'Ernesto drip locations follows Miorandi et al. (2010). Drip discharges estimated assuming an average drip volume of 0.15 ml.

<sup>a</sup> Drip classification after Smart and Freidrich (1987) as modified by Baker et al. (1997).

<sup>b</sup> Named PC-96-7 in Baker et al. (1999b).

<sup>c</sup> Named G1 in Borsato (1997) and Fairchild et al. (2000)

<sup>d</sup> Named G2 in Borsato (1997) and Fairchild et al. (2000)

August 2010 and September 2008 to August 2009, at PC and LBGGM, respectively. The hydrology and hydrochemistry of ERN dripwaters has been well characterised by long-term monthly dripwater and soil water monitoring over the period 1995–2008 (Miorandi et al., 2010). Hydrological and hydrogeochemical background information on each site is given in the supporting information with plots of drip point discharge vs. rainfall data for each site (Figs. S5–S10).

**Table 2**  
Summary of the physical properties of study site soils.

Horizon	Thickness (cm)	Description
<i>Poole's Cavern</i>		
O	4–5	Leaf litter mainly composed of beach, ash and sycamore leaves
A	10–30	Dark brown, lots of thin roots. Horizon thickness varies substantially laterally.
AE	<1	Possible transitional A → E but not prominent
E	5–20	Medium brown clayey horizon penetrated by thick roots and interspersed with limestone fragments.
C	1–20	Light brown. Mainly lime waste and limestone fragments, angular to sub-angular, poorly sorted.
R		Unconsolidated bedrock
<i>Lower Balls Green Mine</i>		
A	10–15	Dark brown, stoneless, silty clay.
AE	1–3	Transitional A → E gradation from dark brown to yellowish brown colour.
E	<10	Yellowish brown horizon. Calcareous, stoney clay.
R		Unconsolidated bedrock.
<i>Grotta di Ernesto</i>		
O	1–5	Leaf litter mainly composed of beach leaves, pine needles.
A	5–10	Dark brown horizon. Thickness varies laterally.
AE	<1	Possible transitional A → E but not prominent
E	>15	Stony brown horizon penetrated by thick roots. Layer is interspersed by unconsolidated, angular–subangular, poorly sorted limestone fragments.
C	>30	Light brown. Mainly weathered limestone and dolomite. Lots of limestone fragments, angular to sub-angular, poorly sorted.
R		Unconsolidated bedrock.

## 2.1. Poole's Cavern

Poole's Cavern (PC), Buxton, UK (53°12'N 1°56'W), is a shallow cave developed in Lower Carboniferous (Asbian) Limestone, Bee Low Limestone Formation, Peak Limestone Group. Vegetation above the cave is secondary deciduous woodland, beneath which an organic-rich top soil has developed (see Hartland et al. (2010a) for a full site description). Poole's Cavern is both unusual and useful because of the coincidence of alkaline and hyperalkaline conditions in a natural cave system, enabling the investigation of the influence of high pH conditions on NOM properties. Hyperalkaline conditions arise because of the dissolution of  $\text{Ca}^{2+}$  and  $\text{OH}^-$  ions in localised lime waste in the overlying soils.

Buxton is located in the Peak District, an upland region in the northern Midlands (mean annual temperature and rainfall 9 °C and 1300 mm, respectively). Atlantic westerlies typically cause a pronounced maximum in effective rainfall in autumn and winter, but in 2008 this effective rainfall was earlier, arriving in late summer (Fig. S5c).

## 2.2. Lower Balls Green Mine

Lower Balls Green Mine (LBGM), Minchinhampton, Gloucestershire, UK (51°7'N, 2°17'W) is a limestone mine abandoned in ca. 1905 that has not been previously studied. The mine was selected to provide data from a site analogous to the well-studied, but currently inaccessible Brown's Folly Mine (BFM), Bath, UK (51°23'N, 2° 22'W) (Baldini et al., 2005; Fairchild et al., 2006a,b). Mining at LBGM was in the Middle Jurassic Inferior Oolite group, Birdlip Limestone Formation, Cleeve Cloud Member (Sumbler et al., 2000). The beds dip gently eastwards with well-developed cross-bedding and are overlain by a rubbly horizon of oolitic marl (Scottsquar member) which is not present 1 km to the west at Upper Balls Green Mine; above the marl is a resistant limestone bed (Harford Member) (Sumbler et al., 2000).

With the exception of a few houses near the mine entrance, land-use above the mine is given over to low-intensity pastoral agriculture. The soil above the site appeared undisturbed with no evidence of ploughing, and is characteristic of the slowly permeable, calcareous, clayey soils of the Evesham group, Sherborne component profile (NSRI, 2008). Minchinhampton (mean annual temperature and rainfall,

**Table 3**  
Summary organic and trace metal composition of sequentially filtered aqueous soil leachates from Lower Balls Green Mine, Grotta d'Ernesto and Poole's Cavern. CC = coarse colloidal, FC = fine colloidal, and ND = nominally dissolved.

Site	Element concentration in size class ( $\mu\text{g L}^{-1}$ )																	
	OC	Si	Na	Mg	Al	Ti	V	Cr	Mn	Fe	Ni	Co	Cu	Zn	Br	Sr	Y	Pb
Lower Balls Green Mine (n=3)	2.2±0.2	1.8±1.2	0.0±2.8	0.2±0.1	975±354	16±14	2.7±1.2	1.8±0.8	9.7±0.5	944±453	0.7±0.2	0.2±0.0	1.4±0.1	54±18	2.7±1.0	1.9±1.4	2.2±0.6	2.9±0.8
Poole's Cavern (n=1)	0.4±0.1	0.0±0.1	0.1±0.6	0.0±0.1	5.0±15	0.0±0.0	0.0±0.0	0.1±0.2	0.0±0.1	6.4±6.8	0.0±0.1	0.0±0.0	0.1±0.1	1.5±4.1	0.7±1.6	0.1±1.1	0.0±0.0	0.0±0.4
Grotta d'Ernesto (n=3)	3.0±0.1	0.4±0.1	4.0±0.5	0.2±0.1	27±14.3	0.1±0.0	0.7±0.8	0.2±0.1	0.1±0.1	1.2±1.5	0.1±0.0	0.0±0.0	0.2±0.0	0.2±4.1	1.3±1.2	7.1±0.4	0.0±0.0	0.3±0.4
	-	0.3	0.2	0.0	129	2.1	0.5	0.2	5.6	111	0.1	-	0.5	33	0.0	0.4	0.3	1.4
	-	0.0	0.2	0.0	10	0.1	0.2	0.1	0.5	5.7	0.0	-	0.4	1.4	0.7	1.0	0.0	0.0
	-	0.2	1.8	0.1	18	0.2	1.1	0.2	0.1	2.8	0.2	-	0.2	0.2	1.2	3.9	0.0	0.0
	0.2±0.5	1.2±2.2	0.0±4.9	0.1±0.3	511±467	6.5±9.5	0.8±0.8	3.6±1.3	13±19	318±329	2.3±5.3	0.3±0.3	1.3±1.2	54±78	3.3±6.2	0.9±8.1	0.8±1.3	1.5±1.0
	3.8±0.5	0.0±0.4	0.4±3.9	0.0±0.3	8.1±4.3	0.1±0.7	0.0±0.6	0.0±0.7	0.9±2.8	7.8±20	0.0±1.8	0.0±0.1	0.0±5.1	24±36	0.4±2.5	0.5±8.8	0.1±0.1	0.1±0.4
	1.7±0.5	0.3±0.3	6.7±2.9	0.1±0.2	32±39	0.3±0.4	0.4±0.5	0.4±0.5	0.6±0.6	4.2±4.1	0.2±1.8	0.0±0.0	0.7±5.0	10±6.8	1.2±1.2	4.3±6.0	0.0±0.0	0.2±0.3
% CC		73	3	41	91	93	58	74	93	96	70	92	64	84	42	15	94	92
CC Rank		10	17	15	7	3	13	9	4	1	11	6	12	8	14	16	2	5
% ND		27	92	52	7	5	39	20	2	1	28	5	22	4	38	76	1	6
ND Rank		7	1	3	10	13	4	9	15	16	6	12	8	14	5	2	17	11

9 °C and 995 mm) is located on the edge of the Cotswold escarpment, an upland limestone region in the south-west English Midlands. The Cotswolds are climatically similar to the Peak District in the north-eastern Midlands, being one of the wettest areas in the region.

The highly permeable limestones of the Inferior Oolite and Great Oolite form major aquifers which feed a multitude of springs, including one which flows from the quarry face above the mine entrance and which forms a stream which extends a short distance into the mine before sinking again. Percolation flow within the mine occurs at numerous points with a range of different flow regimes present, from high-discharge cracks fed directly by spring water, to slow, seepage-flow drips. Speleothem formation occurs throughout the mine and is particularly active in the Macaroni chamber (Fig. S3) in which are numerous incipient stalagmites and flowstones. Surveys of pH and EC of dripwaters in LBGGM were consistent with the expected range for calcite precipitation.

### 2.3. Grotta di Ernesto

Grotta di Ernesto (ERN) located in the Valsugana valley in the Alps of Northeast Italy (45°58'37"N, 11°39'28"E, 1165 m a.s.l.) is, to date, one of the best studied caves in Europe in terms of testing a variety of climate and environmental proxies encoded in its speleothems against a decadal monitoring programme (Frisia et al., 2000; Frisia et al., 2005; Borsato et al., 2007; Miorandi et al., 2010). Grotta di Ernesto develops from about 5 to about 30 m below the surface in dolomitised limestones overlain by Holocene scree deposits containing both limestones and marls onto which an organic-rich, brown calcareous soil, 0.5–1.5 m thick developed. Vegetation above the cave consists of semi-natural conifer vegetation mixed with beech (Fairchild et al., 2009).

The yearly atmospheric precipitation is ca. 1200 to 1300 mm, with two peaks, in May–June and October–November (Borsato et al., 2007). Estimated effective precipitation shows a single peak in October–November, when infiltration is also aided by the reduced foliage cover and strong rainstorms (Borsato et al., 2007).

## 3. Methodology

### 3.1. Dripwater sampling

Dripwater samples were collected from alkaline (pH 7–8) and hyperalkaline (pH 10–13) drip points in Poole's Cavern on a monthly basis over a hydrological year (summer 2008–summer 2009) and additional unfiltered samples were also taken between June and December 2008 from the PE1 drip point (Fig. S2). Samples for colloidal fractions were also taken from LBGGM in September, October and November 2008 and from ERN in November 2008. Sampling campaigns at both LBGGM and ERN were targeted to coincide with hydrologically active periods.

Extensive information on sampling methods and fractionation protocols are available in the supporting documentation accompanying Hartland et al. (2010b). Sample fractionation was achieved by sequential membrane filtration at nominal pore sizes of 1  $\mu\text{m}$  (on site), 100 nm and 1 kDa (in laboratory). Separation at 1 kDa was via ultrafiltration using an Amicon stirred-cell ultrafiltration system at low-flow (4 bar  $\text{N}_2$ ). Materials used in the sampling and filtration of dripwaters were rigorously cleaned using 10%  $\text{HNO}_3$  and Barnstead Nanopure (UHP water,  $18.2 \text{ M}\Omega \text{ cm}^{-1}$ ). Filters were pre-cleaned using 10%  $\text{HNO}_3$  and UHP water in a ratio of 1:3 using the largest practicable volumes given the respective flow-rates. Filters used were Whatman GF/B and Whatman 0.1  $\mu\text{m}$  cellulose nitrate filters, and Millipore 1 kDa regenerated cellulose ultra-filtration membranes. The cleaned Whatman 0.1  $\mu\text{m}$  filters and Millipore 1 kDa membranes were kept in 2%  $\text{HNO}_3$  during storage (1–3 days) and in DIW for 24 h prior to use.

### 3.2. Soil sampling and leaching experiments

Triplicate leaching experiments were performed on samples of the A horizons of soils from above ERN and LBG, and two leaching experiments were conducted with a non-hyperalkaline sample from the A horizon of PC soil. Soils were leached in batches with deionised water (0.04 parts soil to 1 part water); the resulting slurry was immediately filtered at 1  $\mu\text{m}$  and then sequentially filtered at 100 nm and ultrafiltered at 1 kDa (as above). The raw composition of the soil leachates was not analysed because they were too highly concentrated and thus particulate chemistry of the soils was not determined, although it was expected to resemble that of the coarse colloidal fraction.

### 3.3. Instrumental methods

We determined the total organic carbon (TOC) and trace element concentrations in sequentially filtered soil leachates and dripwaters. TOC concentration was determined using a Shimadzu TOC-V, high-temperature combustion analyser following the non-purgable organic carbon (NPOC) method using a 3 minute sparge time and 2 washes between analyses (methods in Hartland et al., 2010b) and trace element concentrations dripwaters were determined using an Agilent quadrupole ICP-MS with a sample matrix of 2%  $\text{HNO}_3$  (methods in Hartland et al., 2011). Fluorescence characterisation of dripwaters was also performed (methods in Hartland et al., 2010b) and colloids in selected dripwater samples were also analysed using transmission electron microscopy (TEM) coupled to X-ray energy dispersive spectroscopy (X-EDS) and by atomic force microscopy (AFM) (methods described in the supporting information).

### 3.4. Classification of operationally derived size classes

In Hartland et al. (2011), colloids and particles in dripwater samples from Poole's Cavern drip point PE1 were subjected to a detailed characterisation of their size, morphology, and composition. Analysis of PE1 dripwater samples (June 2009) using flow field-flow fractionation (FIFFF) and TEM-X-EDS revealed both the heterogeneous composition and poly-disperse distribution of organic-bearing materials with dimensions between 20 nm and  $>1 \mu\text{m}$  (Hartland et al., 2011). The numerically most abundant colloid class were fluorescent, UV-absorbing globular nanoparticles with diameters ranging from 1 to 4 nm, consistent with humic-like colloids characterised in other freshwater environments (e.g. Baalousha and Lead, 2007) (Hartland et al., 2011).

Some data on colloid size and morphology in Poole's Cavern dripwaters have also been presented in Fairchild and Hartland (2010) and Hartland et al. (2010a), and analyses of colloid size and morphology in ERN and LBG dripwaters were also performed using TEM and AFM (Figs. S10 and S11). The results of these various studies are broadly consistent and provide a basis for derivation of generalised colloid classes in dripwaters delineated on the basis of size from sequential filtrations at nominal pore sizes of 1  $\mu\text{m}$ , 0.1  $\mu\text{m}$  (100 nm) and 1 kDa:

- Particulate:  $>1 \mu\text{m}$  (heterogeneous particles)
- Coarse colloidal (CC): 1  $\mu\text{m}$  to 100 nm (large aggregates and globular colloids)
- Fine colloidal (FC): 100 nm to 1 nm (small aggregates, humic-like colloids)
- Nominally dissolved (ND):  $\leq 1 \text{ nm}$  (fulvic-like colloids, organic solutes, free ions, inorganic complexes).

Membrane filters exhibit variable efficiencies and allow a proportion of material to pass with diameters exceeding the assigned 'cut-off' (Lead et al., 1997). Therefore, it is not appropriate to assign sharp boundaries to the size-classes defined. For example, it is expected that fulvic-like colloids with diameters around 1–2 nm may permeate a

1 kDa ultrafilter membrane (Liu and Lead, 2006) although retention efficiency is good and larger material is likely to be retained.

### 3.5. Evapotranspiration calculations

Potential evapotranspiration was calculated for Buxton (PC) and Gloucestershire (LBGM) from January 2008 to August 2009, using the Penman–Monteith equation which is the favoured method for temperate forested environments (Shaw, 1994). Subtraction of potential evapotranspiration (E) from measured rainfall (P) gives an estimate of effective infiltrating precipitation (P–E). Weekly averaged temperature, wind speed, relative humidity and daylight hours were used in the calculations.

## 4. Results

### 4.1. Size-based partitioning of trace elements in aqueous soil leachates and cave dripwaters

#### 4.1.1. Trace element partitioning in soils

The elemental compositions of soil leachates between sites were found to be highly similar, highlighting consistencies in the association of the most surface-reactive metals (e.g. Fe; Milne et al., 2003) with coarse soil organic matter (SOM) and possibly suggesting an atmospheric role in their widespread distribution. One-way analysis of variance (ANOVA Bonferroni means comparison) found no significant differences at the 0.05 level between the population means of each element between sites. Trace elements in the three soils were concentrated in the coarse colloidal fraction, with residual metal being located in the nominally dissolved fraction and little being associated with fine colloids (Table 3). When the proportions of metal associated with the coarse and nominally dissolved size classes in soils were ranked, the following hierarchy of trace metal concentration in the coarse soil fraction was derived: Fe and Y  $>$  Ti  $>$  Mn  $>$  Pb  $>$  Co  $>$  Al  $>$  Zn  $>$  Cr  $>$  Si  $>$  Ni  $>$  Cu  $>$  V  $\gg$  Br  $>$  Mg  $\gg$  Sr  $\gg$  Na (Table 3).

#### 4.1.2. Trace element partitioning in dripwaters

The distribution of trace elements, major ions and organic carbon in sequentially filtered dripwaters from the three study sites also revealed a high degree of uniformity. In Table 4, a representative subset of the size-fractionated dripwater data is presented (remaining data is given Table S2). Two-way ANOVA (Bonferroni means comparison) found no significant difference at the 0.05 level between the population means of each study site, but significant differences were detected (at the 0.05 level) between the population means of Cu, Ni, Co, V and Al in the hyperalkaline PE1 dripwater (PC), and the other studied dripwaters. Trace metals were generally concentrated in the finest size fraction (Table 4), but Co, Cu, and Ni were more evenly distributed between both fine and nominally dissolved size fractions, indicating a colloidal association as previously demonstrated (Hartland et al., 2011).

#### 4.1.3. Comparison between the composition of soils and dripwaters

In essence, the size distribution of metals in the soils (Table 3) was totally different from that found in the dripwaters (Table 4). Results indicate that metals associated with the coarse fraction of soils (Fe, Y, Mn, Pb) were largely not detected in fractionated dripwaters, possibly indicating removal of large colloids and particles by filtration through pore blockage (McCarthy and McKay, 2004).

The alkaline earth metals Na, Mg, and Sr generally show a low affinity for binding at colloid and particle surfaces, although trace amounts are expected to form structural components in aggregates in karstic waters (Shevenell and McCarthy, 2002). For example, the divalent cations Ca and Mg enable the formation of gels through cation-bridging reactions between negatively charged moieties

**Table 4**  
Summary organic and trace metal composition of representative sequentially filtered dripwater samples from Lower Balls Green Mine, Grotta d'Ernesto and Poole's Cavern. Data are averages of triplicate analyses of sequentially filtered dripwater samples. Nd = not determinable, CC = coarse colloidal, FC = fine colloidal, and ND = nominally dissolved. Remaining data in Table S1 (supporting information). Because the concentration of OC in the nominally dissolved fraction was below detection limits, the concentration given represents all organic carbon with a dimension below 100 nm.

Site	Size class	Concentration in size class ( $\text{mg L}^{-1}$ )				Element concentration in size class ( $\mu\text{g L}^{-1}$ )									
		OC	Si	Na	Mg	Al	Ti	V	Cr	Ni	Co	Cu	Br	Sr	
LB1 Lower Balls Green Mine (n = 3)	Particulate	1.6 ± 0.2	0.0 ± 0.2	0.0 ± 0.4	0.0 ± 0.1	0.0 ± 3.0	0.1 ± 0.1	0.0 ± 0.1	-	-	0.0 ± 0.0	0.0 ± 0.1	0.0 ± 2.0	0.0 ± 7.3	
	CC	1.1 ± 0.2	0.22 ± 0.2	0.7 ± 0.4	0.2 ± 0.2	0.0 ± 6.5	0.0 ± 0.1	0.0 ± 0.1	-	-	0.0 ± 0.0	0.1 ± 0.0	4.1 ± 2.2	12 ± 7.1	
	FC	0.1 ± 0.2	0.0 ± 0.1	0.1 ± 0.3	0.0 ± 0.1	2.7 ± 5.9	0.0 ± 0.1	0.0 ± 0.1	-	-	0.0 ± 0.0	0.0 ± 0.1	0.0 ± 1.6	0.0 ± 4.4	
	ND	1.7 ± 0.1	3.0 ± 0.2	7.4 ± 0.2	2.6 ± 0.1	30 ± 0.6	0.7 ± 0.1	0.2 ± 0.0	-	-	0.3 ± 0.0	0.6 ± 0.1	40 ± 1.2	138 ± 3.5	
LB3 Lower Balls Green Mine (n = 3)	Particulate	1.9 ± 0.2	0.1 ± 0.2	0.1 ± 0.3	0.0 ± 0.1	0.6 ± 0.8	0.0 ± 0.1	0.0 ± 0.0	-	-	0.0 ± 0.0	0.0 ± 0.0	0.0 ± 2.0	3.2 ± 7.8	
	CC	1.3 ± 0.1	0.0 ± 0.3	0.1 ± 0.5	0.0 ± 0.2	0.0 ± 2.5	0.0 ± 0.1	0.0 ± 0.0	-	-	0.0 ± 0.0	0.0 ± 0.1	0.3 ± 3.5	0.0 ± 11	
	FC	1.2 ± 0.2	0.0 ± 0.3	0.0 ± 0.6	0.0 ± 0.2	0.0 ± 3.2	0.0 ± 0.1	0.0 ± 0.0	-	-	0.0 ± 0.0	0.0 ± 0.1	0.0 ± 3.9	2.0 ± 11	
	ND		3.0 ± 0.1	7.3 ± 0.2	2.8 ± 0.1	31 ± 2.1	0.6 ± 0.1	0.1 ± 0.0	-	-	0.3 ± 0.0	0.3 ± 0.1	43 ± 2.2	149 ± 3.0	
BC1 Poole's Cavern (n = 3)	Particulate	0.8 ± 0.3	0.0 ± 0.1	0.0 ± 0.1	0.0 ± 0.1	0.0 ± 0.9	0.0 ± 0.1	0.0 ± 0.1	0.2 ± 0.2	-	0.0 ± 0.0	0.0 ± 0.6	1.2 ± 1.4	1.7 ± 2.1	
	CC	0.4 ± 0.3	0.2 ± 0.1	0.6 ± 0.1	1.1 ± 0.0	0.4 ± 1.0	0.0 ± 0.1	0.0 ± 0.0	0.0 ± 0.0	-	0.0 ± 0.0	0.3 ± 0.6	1.6 ± 1.8	1.1 ± 1.9	
	FC	0.7 ± 0.4	0.0 ± 0.0	0.0 ± 0.1	0.0 ± 0.0	0.3 ± 1.3	0.0 ± 0.1	0.0 ± 0.0	0.0 ± 0.0	-	0.0 ± 0.0	0.1 ± 0.0	1.0 ± 1.6	0.9 ± 1.8	
	ND		2.7 ± 0.0	3.1 ± 0.0	0.9 ± 0.0	5.3 ± 1.0	0.7 ± 0.1	0.4 ± 0.0	0.2 ± 0.0	-	0.3 ± 0.0	0.2 ± 0.0	40 ± 0.8	56 ± 1.0	
PE1 Poole's Cavern (n = 3)	Particulate	1.5 ± 0.3	0.0 ± 0.1	0.0 ± 0.1	-	124 ± 39	0.8 ± 0.1	0.0 ± 0.8	0.0 ± 0.3	0.1 ± 0.1	0.0 ± 0.0	0.4 ± 0.1	0 ± 1.2	0 ± 2.2	
	CC	0.3 ± 0.3	0.4 ± 0.1	0.2 ± 0.1	-	325 ± 39	0.1 ± 0.1	1.7 ± 0.9	0.2 ± 0.4	0.0 ± 0.1	0.1 ± 0.0	0.0 ± 0.2	0.6 ± 1.5	6.4 ± 2.6	
	FC	0.5 ± 0.2	3.3 ± 0.2	0.1 ± 0.2	-	26 ± 55	0.0 ± 0.1	0.9 ± 1.4	0.7 ± 0.6	0.1 ± 0.2	0.1 ± 0.1	0.4 ± 0.3	1.3 ± 1.4	0.9 ± 2.4	
	ND	1.4 ± 0.1	3.2 ± 0.2	3.7 ± 0.2	-	808 ± 54	0.8 ± 0.1	20 ± 1.3	8.9 ± 0.5	0.8 ± 0.2	0.5 ± 0.1	1.2 ± 0.3	32 ± 1.0	54 ± 2.0	
St-1 Grotta d'Ernesto (n = 1)	Particulate	1.2 ± 0.2	0.1 ± 0.4	0.0 ± 0.0	0.1 ± 0.1	1.6 ± 1.5	0.0 ± 0.1	0.0 ± 0.1	0.01 ± 0.0	0.0 ± 0.0	0.0 ± 0.0	0.0 ± 0.0	0.3 ± 0.5	0.3 ± 0.2	
	CC	0.5 ± 0.6	0.0 ± 0.1	0.1 ± 0.0	0.1 ± 0.1	0.0 ± 1.5	0.0 ± 0.0	0.0 ± 0.0	0.0 ± 0.0	0.0 ± 0.0	0.0 ± 0.0	0.0 ± 0.1	0.1 ± 0.5	0 ± 0.5	
	FC	0.5 ± 0.6	0.1 ± 0.1	0.0 ± 0.0	0.1 ± 0.2	1.8 ± 1.4	0.0 ± 0.1	0.0 ± 0.0	0.0 ± 0.0	0.0 ± 0.0	0.0 ± 0.0	0.1 ± 0.1	0.9 ± 0.4	0.2 ± 0.6	
	ND	1.6 ± 0.1	2.4 ± 0.7	0.4 ± 0.0	4.3 ± 0.1	6.2 ± 0.7	0.6 ± 0.0	0.1 ± 0.0	0.1 ± 0.0	0.1 ± 0.0	0.1 ± 0.0	0.2 ± 0.1	4.8 ± 0.2	19 ± 0.5	
St-ER78 Grotta d'Ernesto (n = 1)	Particulate	0.4 ± 0.3	0.0 ± 0.1	0.0 ± 0.0	0.2 ± 0.2	0.0 ± 1.3	0.0 ± 0.0	0.0 ± 0.0	0.0 ± 0.0	-	0.0 ± 0.0	0.0 ± 0.0	0.3 ± 0.4	0.0 ± 0.8	
	CC	0.8 ± 0.3	0.1 ± 0.1	0.0 ± 0.0	0.2 ± 0.1	2.3 ± 1.2	0.0 ± 0.0	0.0 ± 0.0	0.0 ± 0.0	-	0.0 ± 0.0	0.0 ± 0.0	0.3 ± 0.3	1.1 ± 0.2	
	FC	0.5 ± 0.6	0.0 ± 0.1	0.0 ± 0.0	0.0 ± 0.1	0.0 ± 1.9	0.0 ± 0.0	0.0 ± 0.0	0.0 ± 0.0	-	0.0 ± 0.0	0.0 ± 0.0	0.8 ± 0.2	0.0 ± 0.5	
	ND	2.1 ± 0.6	2.1 ± 0.0	0.4 ± 0.0	5.3 ± 0.1	7.7 ± 0.7	0.6 ± 0.0	0.1 ± 0.0	0.1 ± 0.0	-	0.1 ± 0.0	0.2 ± 0.0	6.3 ± 0.2	17 ± 0.1	
	% CC	5	7	11	33	21	8	4	7	9	21	5	6		
	CC rank	10	7	4	1	3	6	12	8	5	2	11	9		
	% ND	79	92	88	65	78	88	89	78	84	65	93	94		
	ND rank	8	3	6	11	9	5	4	9	7	10	2	1		

(Verdugo et al., 2008), possibly explaining the relatively greater partitioning of Mg into the coarser classes over Sr.

In natural waters, small colloids are typically present in numbers, which are orders of magnitude greater than particulates (e.g.  $10^6$  times more 10 nm colloids than the equivalent number of 1  $\mu\text{m}$  particles) (Doucet et al., 2007). Preferential partitioning of surface-reactive trace metals into the finest size-fraction may be predicted based on the greater available surface area for sorption (Buffle et al., 1998) and this is consistent with the data from fractionated dripwaters (Table 4).

#### 4.2. Competitive binding of metals by NOM in soils and dripwaters

Trace metal binding by NOM in dripwaters was modelled using the Windermere Humic Aqueous Model (WHAM) 6.1 which incorporates Model VI (Tipping, 1998), and visual MINTEQ 3.0 which incorporates the NICA-Donnan model (Kinniburgh et al., 1999). Modelling of metal binding to NOM in natural water samples is challenging because of the extreme heterogeneity of the OM present which encompasses a complex mixture of compounds with variable binding affinities and physiochemical properties including, variable charge and binding site distributions (Filella, 2008). This is further complicated by the variable stoichiometry of the reaction and competition between metals for binding sites (Unsworth et al., 2006). Model VI is based on a discrete set of sites (Tipping, 1998), whereas the NICA-Donnan model employs a bimodal, continuous distribution for protons and metal ions (Kinniburgh et al., 1999); but both employ semi-empirical electrostatic corrections to cation binding.

Four representative drip points were chosen and the samples with the lowest recorded TOC concentrations were selected. For the purposes of the modelling exercise all organic carbon in the sample was presumed to be colloidal humic acid (HA) and we focused on the transition metals Al(III), Cr(III), Fe(II), Co(II), Ni(II), Cu(II) and Zn(II) (Fig. 1). This simplification is justified because standard models of cation binding cannot fully reproduce the properties of NOM ligands (Filella, 2008), rather we sought to evaluate whether metal binding to organic matter is expected at the ambient concentrations encountered. Inorganic colloidal phases were not included because during most of the monitoring, Fe and Mn were below detection limits ( $0.5 \mu\text{g L}^{-1}$  and  $0.2 \mu\text{g L}^{-1}$ , respectively) and colloid characterisation by TEM-X-EDS did not identify abundant inorganic colloids in the studied samples (Fig. S10).

As shown elsewhere (Unsworth et al., 2006), estimations of HA-metal binding between the models were quite variable, but both models predicted that a proportion of each metal would be bound to HA under the given conditions (except where no metal was measured – marked by \*; Fig. 1). Model predictions were most consistent for Cu(II), the speciation of which was generally predicted to be dominated by binding to HA. In general, WHAM predicted higher proportions of Al(III) bound to HA, while MINTEQ predicted higher HA binding of Fe, Ni, Co and Zn (Fig. 1).

The predicted binding of Cu(II) was most uniform between models and across study sites (Fig. 1). Cu(II) is known to strongly compete for binding sites in humic substances (Marang et al., 2009) and Cu has been shown to be well correlated with Ni and Co in PE1 dripwater (Hartland et al., 2011), consistent with complexation of Cu, Ni and Co by NOM at high pH, as shown by diffusive gradients in thin films (DGT) (Hartland et al., 2011). The same study also identified unusually strong complexation of Co; this apparent anomaly can be reconciled with greater competitive binding by Cu and Ni [indicated by elevated Cu/OC and Ni/OC at high pH compared to Co/OC at this site (Fairchild and Hartland, 2010)], by considering a mixture of NOM complexation patterns for these metals, i.e. all three metals compete for certain sites, but Cu and Ni compete for a wider range of binding sites than Co, in particular for coarse SOM (see later).

We directly compared the concentration of Cu to that of the other, ubiquitous metals, Co and Ni, in the fractionated cave dripwaters and aqueous soil leachates and annual mean rainfall concentrations at Holme Moss (HM), UK between 2007 and 2009 (Fig. 2 and Table 5). The competitive affinity of these metals for functional groups in NOM is considered to be of the order:  $\text{Cu} > \text{Ni} > \text{Co}$ , and this affinity is expected to be enhanced at pH 8, with Cu out-competing other metals for suitable binding sites (Milne et al., 2003; Marang et al., 2009; Fairchild and Hartland, 2010). This hierarchy of binding affinity is particularly well characterised for purified humic extracts and is considered to be essentially uniform between humic and fulvic acids (Milne et al., 2003).

When considered in their entirety, concentrations of Cu, Ni and Co in dripwaters were well correlated across study sites showing a consistent increasing trend (Fig. 2a and b). This consistency, particularly in Cu:Ni may indicate a common mechanism driving their changing abundance in dripwaters (although some scatter is expected since not all of the metal ions will be present in complexes with NOM). Model predictions of Ni and Co binding to HA indicated that only a minor fraction of the Ni and Co in dripwaters would be complexed with HA (Fig. 1). However, it is well documented that uncertainties in model predictions increase for metals with lower binding affinities for NOM (e.g. NICA-Donnan; Groenenberg et al., 2010), and that these uncertainties primarily originate from the considerable compositional differences between purified humic extracts used to calibrate equilibrium models (Milne et al., 2003) and NOM found in environmental samples (Unsworth et al., 2006; Filella, 2008; Groenenberg et al., 2010).

Although sophisticated, equilibrium binding models rely on our poorly developed understanding of NOM composition and function (Filella, 2008), but the *relative* binding affinity of metal ions for humic and fulvic acids is better defined (Milne et al., 2003). Because metal binding with NOM is governed by a competitive hierarchy of binding affinity (Kinniburgh et al., 1999; Marang et al., 2009), it is reasonable to expect (assuming that metal is present mainly in complexes with NOM) that the relative abundance of metals will reflect this hierarchy. Total Cu vs. Ni and Cu vs. Co concentrations in dripwaters were consistent with the order of competitive binding affinity  $\text{Cu} > \text{Ni} > \text{Co}$  (Fig. 2a and b). Furthermore, Cu:Ni in HM rain was similar to that in dripwaters (Fig. 2a), although Cu to Co ratios in rain were substantially lower (Table 5), possibly indicating mobilisation of Co during infiltration.

In Fig. 2c and d, the Cu vs. Ni and Cu vs. Co linear regression trend lines for dripwaters are plotted with the predicted Cu vs. Ni and Cu vs. Co trends derived from the equivalent ratios of  $n_1$  binding affinity parameters for humic acid (HA) and fulvic acid (FA) from the study of Milne et al. (2003). The  $n_1$  value is a generic parameter which describes the variation in hydrolysis behaviour of metals as an indicator of their potential for binding to humic substances, it is derived as a function of the formation of the first hydrolysis complex ( $\text{MOH}^{(z-1)+}$ ) for a given metal ion ( $\text{M}^{z+}$ ) and does not differ between humic and fulvic acids (Milne et al., 2003). Humic and fulvic affinity trend lines were derived by taking the equivalent  $n_1$  ratio, e.g.  $\text{Co/Cu} = 0.71/0.53 = 1.34$ , and iteratively calculating the proportion of Cu expected for a given amount of Co, i.e.  $\text{Cu} (\mu\text{g L}^{-1}) = \text{Co} (\mu\text{g L}^{-1}) \times 1.34$  (Fig. 2d). The advantage of this approach is that it requires no prior knowledge of the proportions of HA/FA in NOM, the NOM concentration, or of metal complexation patterns, since the *relative* amount of each metal (which are presumed to be in direct competition for binding sites) is a function of their competitive interaction (binding affinity), which is uniform for metal binding to both HA and FA (Milne et al., 2003). It should be noted that this relationship may break down at higher metal loading due to the effect of concentration on competition (Tipping, 2001) as may be seen in Fig. 2c (orange dashed line).

Interestingly, during periods of high infiltration, metal ratios in samples taken from ERN drips St-1 and St-2 and PC drip PE1 showed marked shifts toward higher values of Cu:Ni and Cu:Co. But while Cu

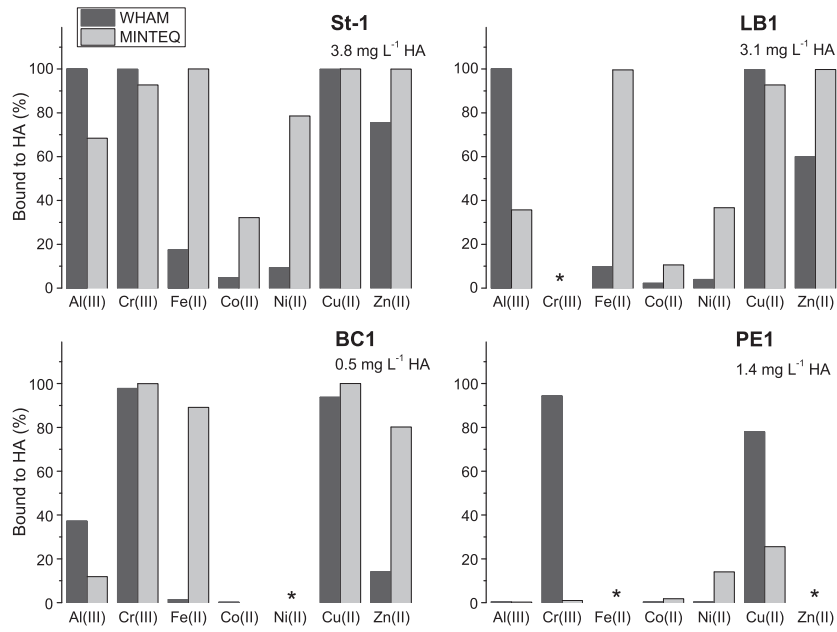


**Fig. 1.** Results of equilibrium speciation modelling using WHAM 6.1 and MINTEQ 3.0 based on the simplification that the metal binding component of natural organic matter in dripwater was colloidal humic acid. Samples from four representative drip points were modelled (BC1 and PE1, PC; LB1, LBGm; and St-1, ERN). Samples selected were those with the lowest recorded total organic carbon concentration.

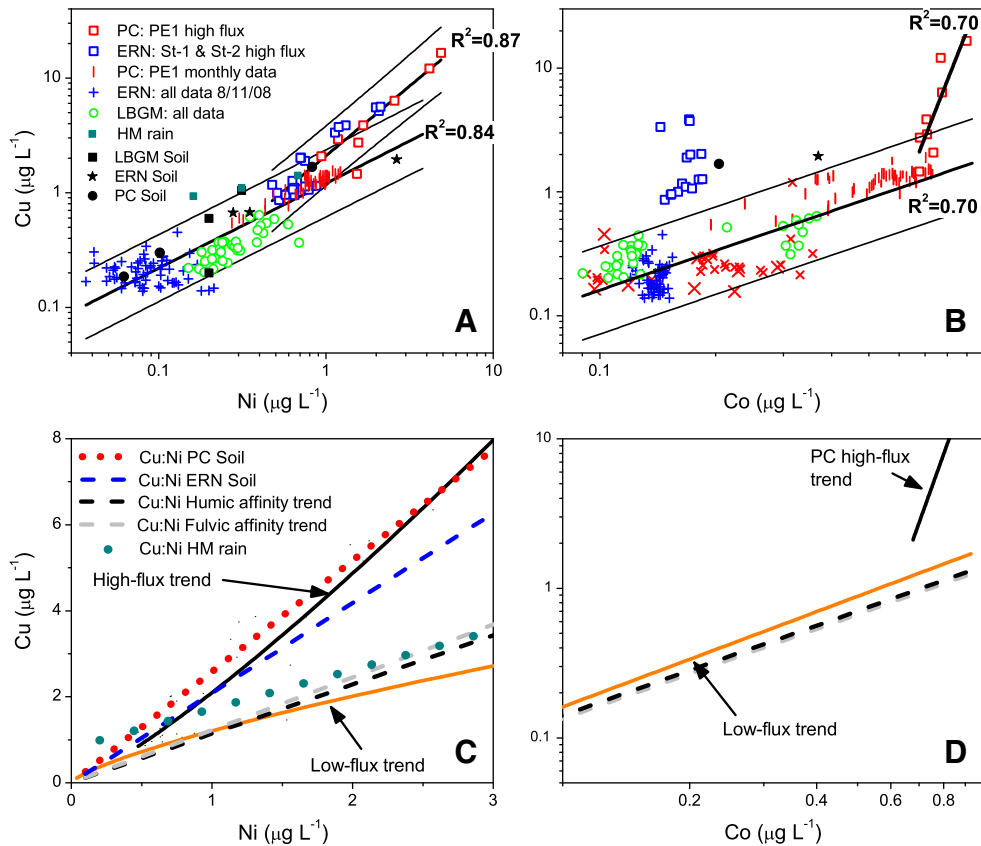


**Fig. 2.** Inferred competitive binding of Cu, Ni and Co by humic-like natural organic matter (NOM) and coarse soil organic matter (SOM) in cave dripwaters. Plots show linear regressions of metal concentrations in dripwaters (a) Cu vs. Ni, and (b) Cu vs. Co. Plots in (c) and (d) show predicted metal ratios (c) Cu:Ni, and (d) Cu:Co, based on the equivalent  $n_1$  NICA-Donnan humic and fulvic binding affinity ratio ( $n_1$  values from Milne et al., 2003). Plot (c) also shows the equivalent Cu:Ni trend lines calculated using the average Cu:Ni in the Poole's Cavern (PC) and Grotta di Ernesto (ERN) soil leachates and in Holme Moss (HM) rainwater. Ratios of Cu to Ni in dripwaters show increased similarity to ratios in soils at times of high organic carbon and trace metal flux, indicative of qualitative changes in NOM composition (i.e., more aromatic/hydrophobic SOM). Thin lines in (A) and (B) are 95% confidence bands from linear regressions. (For interpretation of the references to colour in this figure legend, the reader is referred to the web version of this article.)



**Table 5**  
Volume-weighted annual mean rain trace metal concentrations in  $\mu\text{g L}^{-1}$  from Holme Moss, UK, between 2006 and 2009 (Source: Defra, 2012). LOD = limit of detection.

Year	LOD	Al	Ti	V	Cr	Mn	Fe	Ni	Co	Cu	Zn	Sr	Cd	Ba	Pb
		0.6	0.04	0.02	0.04	0.006	1	0.01	0.006	0.02	1	0.03	0.002	0.06	0.06
2007		11.30	0.31	0.47	0.18	1.46	17.03	0.31	0.05	1.11	9.71	2.19	0.03	1.21	1.42
2008		9.50	0.17	0.33	0.10	1.27	10.88	0.19	0.04	0.93	6.25	1.95	0.02	1.05	0.91
2009		10.03	0.25	0.36	0.15	2.15	12.11	0.73	0.04	1.42	8.60	2.21	0.02	1.45	1.54

and Ni concentrations increased linearly at these times, Co concentrations did not increase appreciably (Fig. 2a–b). These shifts coincided with elevated TOC concentrations and increases in the concentration of metals (Fe, Al, Ti, and Y) which showed an association with the coarse fraction of soils (Section 4.1.1). During these higher fluxes of NOM and metals, Cu:Ni departed from the characteristic range for binding to humic and fulvic acids (Fig. 2c and d), but remained well correlated. Indeed, Cu:Ni at both ERN and PC were very similar (Fig. 2a) and were close to the Cu:Ni measured in the soil leachates from these sites (Fig. 2c).

Soil and rain Cu:Ni trend lines were derived in the same way as humic and fulvic affinity lines (see above), but were calculated based on the average Cu:Ni in the PC and ERN soil leachates and HM rainwater (Fig. 2c). It is clear that Cu:Ni ratios in dripwaters at times of elevated NOM and metal flux show increased similarity to the ratio measured in the soils (Fig. 2c). At these times, Cu:Ni departed from values characteristic of binding to HS, and notably, from the Cu:Ni measured in HM rainwater (green dotted line, Fig. 2c), possibly consistent with direct contributions of humic-like NOM and metals from rainfall (Nimmo and Fones, 1997; Muller et al., 2008).

Thus, during periods of high NOM flux, increases in Cu:Ni are argued to reflect changes in the competitive interaction between Cu and Ni ions, i.e. Cu shows an increased affinity for binding at sites in (more aromatic) SOM compared to Cu vs. Ni binding with humic-like NOM (Fig. 2c). This is considered to be indicative of a qualitative change in NOM composition to relatively higher aromaticity/hydrophobicity and is consistent with the strongly competitive nature of Cu(II) binding (Marang et al., 2009). In contrast, the Cu:Co ratios in ERN and PC dripwaters during high-flux events (Fig. 2b) were not correlated with each other and Co did not increase in concentration, therefore leading to the conclusion that Co did not compete (or was out-competed) for binding sites in SOM.

#### 4.3. Relation between hydrology and NOM–metal transport

In the following section, we present the results of temporal monitoring of NOM and metal concentrations in cave dripwaters. However, because of the large amount of data acquired only those results considered to be of the greatest hydrogeochemical significance are presented and discussed (full dataset in Tables S3–S18).

In our analysis we do not address the potential array of processes occurring during the flow through the karst aquifer. Most important among these is the potential for highly reactive metals to transfer between phases, e.g. adsorb to aquifer surfaces. In general, desorption timescales are much longer than the equivalent forward reactions between metals and humic substances (Tipping, 2001). In respect to NOM–metal complexes in PE1 dripwater (PC), desorption for Cu, Ni, Co and V bound to the fine colloidal and dissolved fractions occurs very slowly, e.g. given the availability of suitable binding sites complete desorption of very strongly bound metals (e.g. Cu, Ni, Co) may take several weeks to occur (Hartland et al., 2011).

During the sampling campaigns at ERN and PC, additional non-fractionated samples were taken during the most hydroclimatologically active periods. At ERN, logistical constraints meant that collection and size-fractionation of dripwaters could only be performed at the end of the sampling campaign (to limit the potential for aggregation of colloids) and so additional raw dripwater samples were collected from

the high discharge drips St-1 and St-2 between 4/11/08 and 7/11/08. At PC, additional unfiltered samples were also taken from drip PE1 on an approximately weekly basis through the period June 2008 to November 2008 in addition to the monthly size-fractionated samples. Thus, the PE1 drip was studied in the greatest detail and is given the most attention here.

##### 4.3.1. Lower Balls Green Mine, September 2008–December 2008

The monitored drip sites of LBGm were characterised by very high mean discharges, but quite low coefficients of variation (Table 1). An analysis of the discharge–rainfall relationship in drips LB1–3 showed that drip point LB1 was best correlated with antecedent rainfall (Fig. S9a). Size fractionated samples were obtained from LBGm drip points in September, October, and November 2008 and analysed for TOC, fluorescence and trace elements. Effective rainfall during the preceding July and August was high, but this was followed by a dry September and wet October and November (Fig. S8d). Over this time, the discharge of drip points LB1 and LB2 was higher than at any other time between January 2008 and August 2009, but drip point LB3 showed little variation in response to rainfall (Fig. S8).

Between September and December 2008, organic carbon in LBGm dripwaters was most variable in drips LB1 and LB3, fluctuating between 3.06 and 7.40  $\text{mg L}^{-1}$ , and 2.50 and 6.40  $\text{mg L}^{-1}$ , respectively. Organic carbon (OC) concentration in LB2 dripwater varied in the range 2.70 to 5.60  $\text{mg L}^{-1}$  with most OC being present in the particulate (36%) and coarse colloidal (31%) size classes, the remainder being split evenly between the fine (17%) and nominally dissolved fractions (16%). Similarly, OC in LB3 dripwater was found predominantly in the particulate (39%) and coarse colloidal (39%) size range with only 22% in the nominally dissolved size class.

Despite the large proportions of OC in the particulate and coarse colloidal size classes in LB2 and LB3 samples, the transition metals Co, Cu and Ni did not partition into the larger size-classes, being concentrated in the nominally dissolved fraction and showing no temporal variability. In contrast to drips LB2 and LB3, the partitioning of OC and trace metals at LB1 revealed large changes between months (Fig. 3). The concentration of organic carbon and metals (Cu, Ni, Co) in the nominally dissolved size class declined steadily between September and November 2008. This decline was matched by an increase in the concentration of OC and Cu, Ni and Co in the coarse colloidal and particulate size classes in the wetter period (Fig. 3). In particular, Co and Ni showed strong shifts into the particulate size range in October and November 2008.

These changes in metal and NOM partitioning coincided with increases in the concentration of Zn and Fe in November 2008. The proportions of Fe and Zn in each size class could not be determined because of variable release of these metals from filters (Hartland et al., 2011), but based on the strong tendency of Fe to partition into the coarse size class in soils (Table 3), and the similarity of Zn binding affinity to Cd and Cu (Companys et al., 2007; Warnken et al., 2007), this arguably represents an increase in metal transport by coarse colloids and particulates. Hence, these results indicate that NOM and trace metals in LB1 dripwater in the nominally dissolved and coarse colloidal/particulate size classes displayed divergent hydrological behaviour in response to increased infiltration and that metal transport by particles occurred preferentially to fine colloids.

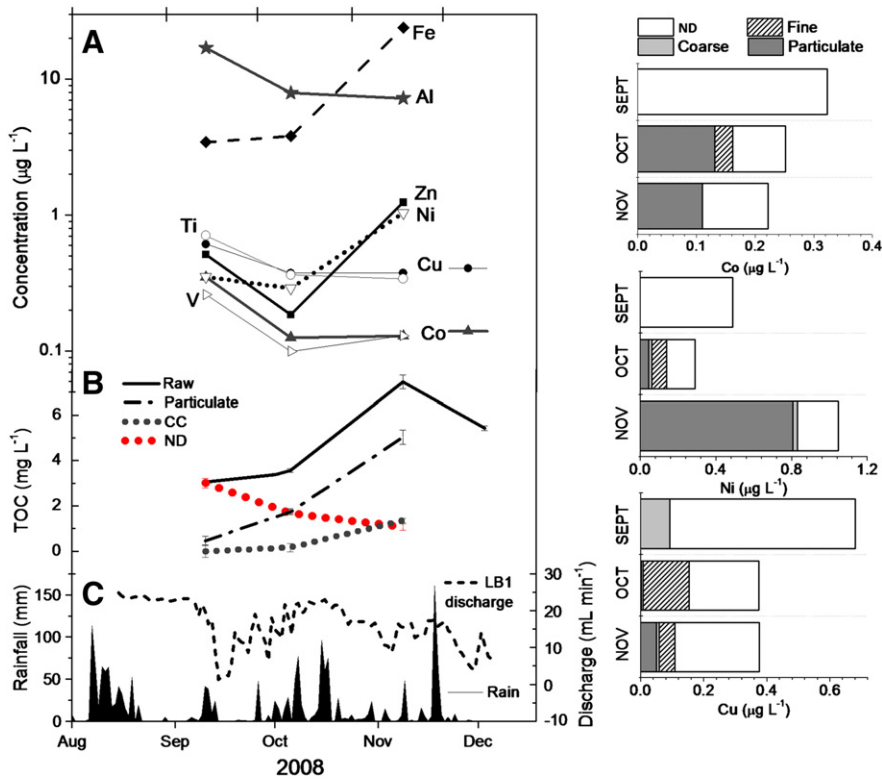


**Fig. 3.** Time series of (a) trace metal concentrations in raw LB1 dripwater samples. (b) total organic carbon (TOC) concentration in sequentially filtered LB1 dripwater and (c) daily rainfall and drip discharge for Lower Balls Green Mine drip LB1. Stacked bars show metal distribution between colloidal size classes in September, October and November 2008 for transition metals Cu, Ni and Co.

4.3.2. Grotta di Ernesto, 3/11/2008–8/11/2008

Fieldwork was carried out at ERN in both October 2007 and November 2008. The 2007 field campaign was conducted before the first winter rains of that year and raw concentrations of Cu, Al and Mn (2.67, 2.99 and 0.28  $\mu\text{g L}^{-1}$ , respectively (other metals were not measured)) in dripwater samples were substantially lower than in November 2008 (Fig. 4). Drip rates, pH and electrical conductivity (EC) values at Grotta di Ernesto were monitored on a daily basis over the period 4/11/08–8/11/08. The first heavy rainfalls of the winter occurred on 28/10/08 and were followed by a larger storm lasting from 1/11/08 to 4/11/08 (Fig. 4d). Variations in drip rate, EC and pH were consistent with discharge of stored waters and mixing (dilution) with lower EC rainwater in the days following the peak rainfall event (Tooth and Fairchild, 2003) (Fig. 4b). The response was quickest in drip points St-1 and St-2, consistent with the greater proportion of fracture-fed flow in these drips (Miorandi et al., 2010). Drip points St-ER78 and St-ER77 were slower to respond, signifying a piston-flow (or, pressure pulse) response characteristic of the flow-routing of these drips (Miorandi et al., 2010).

In Fig. 4 the concentrations of trace metals (Al, Mn, Ni, Cu, and Co) and OC in drip St-1 are plotted against rainfall and drip rate variations between 1/11/08 and 11/11/08. Organic carbon, fluorescence and metals (Al, Mn, Ni, and Cu) in St-1 dripwater peaked in concentration on 4/11/08 and declined thereafter. Higher humic- and fulvic-like fluorescence intensities were also accompanied by transient peaks in tryptophan-like (peak T) fluorescence intensity. Thus, the coincidence of elevated concentrations of transition metals with higher NOM concentrations and fluorescence intensities (which originate mainly from the ca. 1 kDa fraction (Hartland et al. (2010b))) are indicative of simultaneous transmission of particulates, fine colloids and DOM.

4.3.3. Poole's Cavern, June 2008–August 2009

The dripwaters of Poole's Cavern were monitored on a monthly basis from summer 2008 to summer 2009. Data from the normal-

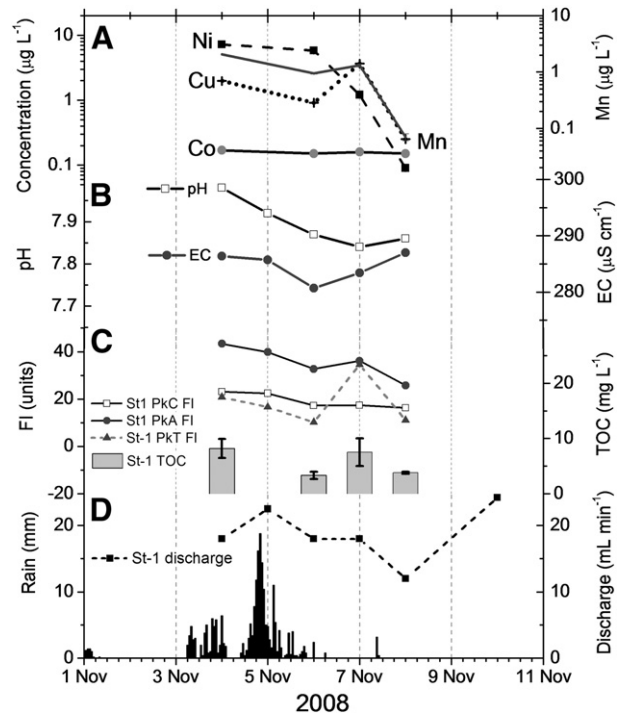


**Fig. 4.** Time series of Grotta d'Ernesto drip St-1 from fieldwork conducted in November 2008 (a) elemental concentrations in raw samples, (b) variations in pH and electroconductivity, (c) total organic carbon (TOC) concentration and fluorescence intensities and (d) daily rainfall and drip discharge. PKC FI = Peak C fluorescence intensity (excitation 300–350 nm; emission 400–460 nm); PKA FI = Peak A fluorescence intensity (excitation 230–260 nm; emission 400–460 nm); and PKT FI = Peak T fluorescence intensity (excitation 220–235 nm; emission 330–370 nm).

pH drips BC1 and BC2 showed strong co-variation in Co, Ti and V over this period, consistent with correlations between these metals (Co and Ti,  $R^2=0.67$ ; Co and V,  $R^2=0.69$ ). Organic carbon and trace metals (Co, Ti and V) in BC1–2 samples fluctuated in the range of  $1\text{--}4\text{ mg L}^{-1}$  and  $0.1\text{--}1\text{ }\mu\text{g L}^{-1}$ , respectively. As found in LBG drip samples LB2 and LB3, a greater proportion of NOM was present in the particulate size class during the wetter months, but no pronounced differences in trace metal partitioning between size classes were observed between seasons.

Analysis of variance of the elemental composition of size-fractionated BC1 and BC2 samples found no statistically significant difference at the 0.05 level (ANOVA, Bonferroni test) between August–December 2008 compared to January–August 2009. Indeed, the distribution of V, Co and Ti between size classes in BC1–2 samples was remarkably consistent. All three metals were predominantly associated with the nominally dissolved size class (V ca. 75%, Ti ca. 87–95% and Co ca. 81–83%) with small proportions associated with the fine and coarse fractions. Size-based partitioning of Co, Ti and V in the alkaline drips BC1–2 was substantially similar to that found in the hyperalkaline dripwater PE1, possibly pointing to their common complexation by NOM in the nominally dissolved size class.

Of all the dripwaters studied, those of hyperalkaline drip point PE1 were studied in the greatest detail. As discussed in Fairchild and Hartland (2010), competitive binding of Cu and Ni > Co at high pH values (pH 9–13) in PC dripwaters is reflected in elevated metal:OC compared to lower pH drips (e.g. BC1–2); Cu:OC and Ni:OC increase from ca. 0.1 to 1.5% at between pH 8 and 12 at this site (Fairchild and Hartland, 2010).

Detailed characterisation of colloids and particles in PE1 dripwater sampled in June 2009 showed that small, globular colloids with diameters between ca. 1 and 4 nm were the most abundant colloid class, and NOM in this size range was shown to fluoresce strongly at 320 nm excitation, characteristic of humic-like compounds (Hartland et al., 2011). Furthermore, the fluorescence signal in PC dripwater samples is strongest in the nominally dissolved fraction, supporting the interpretation that the smallest fulvic-like colloids readily penetrated the 1 kDa ultra-filter membrane (Hartland et al., 2010b). In Fig. 5, the concentration and fluorescence attributes of NOM in size-fractionated PE1 samples are plotted against variations in rainfall and effective precipitation over the study period.

During peak effective rainfall in August and September 2008, organic carbon concentration in raw PE1 samples was substantially elevated (Fig. 5d), but because of colloidal and particulate inner-filtering (Hartland et al., 2010b), fluorescence was not similarly elevated in raw samples (Fig. 5a–b). Peak C emission wavelengths were also substantially altered following filtration, consistent with disruption of peak C fluorescence by the coarse fraction. The mean peak C emission wavelength in fractionated samples is given (Fig. 5c) as an indicative measure of NOM composition since peak C emission wavelength is correlated with aromaticity/hydrophobicity (Senesi et al., 1991; Baker et al., 2008). Thus, the data indicate that NOM in PE1 dripwater during August–October 2008 was relatively more aromatic/hydrophobic than in later months.

Relative to the changes in TOC concentration, fluorescence intensities in the fine and nominally-dissolved size range were slower to increase following infiltration events, only increasing as particulate TOC concentration, and peak C emission wavelengths declined (Fig. 5). In Fig. 6, the concentration of trace metals in raw samples, fine and nominally dissolved size classes is shown. Concentrations of Ti, Fe, Ni and Cu, as well as Mn and Zn in raw samples were markedly elevated in the period July–November 2008 (Fig. 6c–g) and showed three distinct spikes in concentration. The concentration of Cu, Ni and Ti in the fine and nominally dissolved size classes meanwhile was essentially unaltered, indicating that Cu, Ni and Ti were mobilised in association with particulate NOM. This inference is supported by higher Cu:Ni in these samples (Fig. 2a and c), consistent with transmission of highly aromatic, coarse soil organic

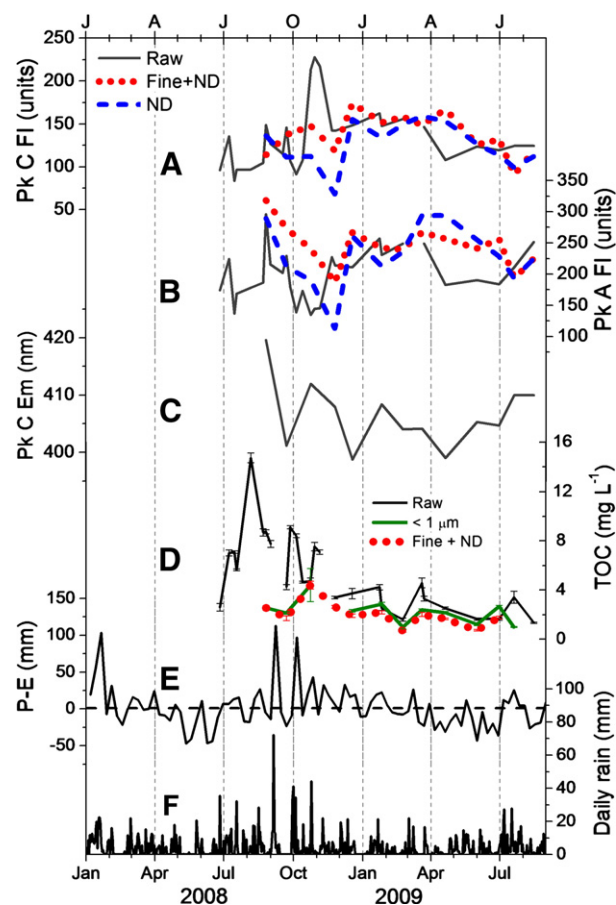
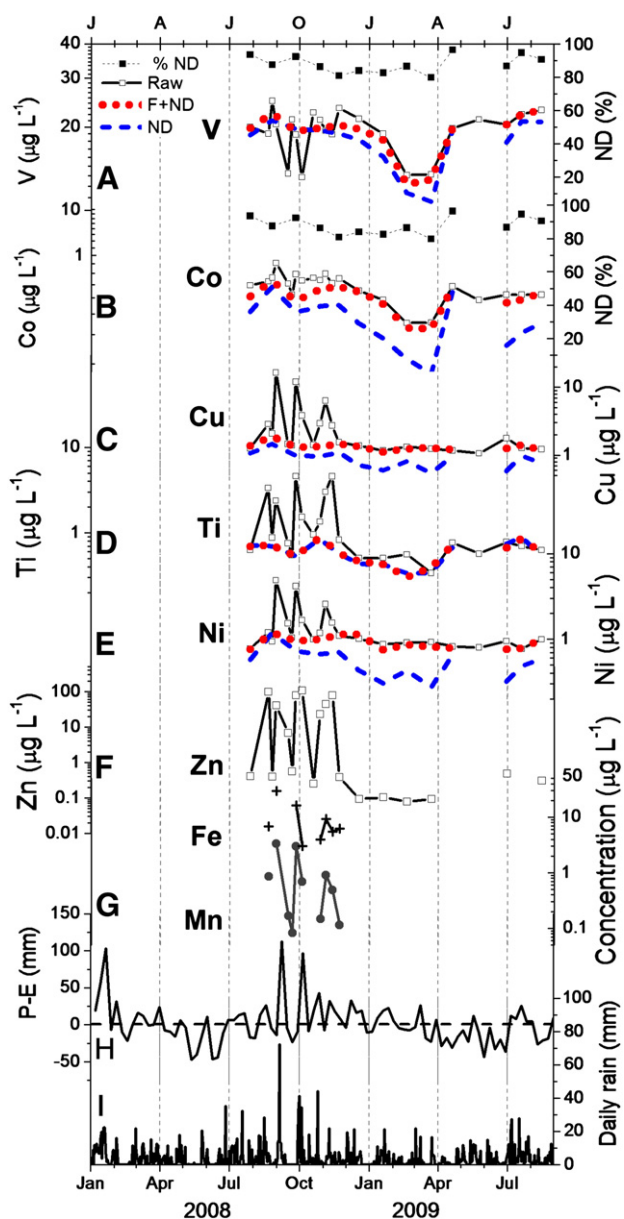


Fig. 5. Time series of NOM fluorescence attributes and organic carbon concentrations in sequentially filtered PE1 dripwater samples collected between June 2008 and August 2009. FI = fluorescence intensity (Raman-corrected), EM = emission wavelength, TOC = total organic carbon, and P – E = actual precipitation minus potential evapotranspiration (Penman). ND = nominally dissolved.

matter (SOM). Increases in the concentration of Zn, and the transient presence of Mn and Fe in PE1 dripwater, provide further evidence for the ephemeral transmission of particulate SOM in pulses in response to peaks and troughs in effective rainfall (Fig. 6d and g).

Strongly contrasting with the behaviour of Cu, Ni, Ti, Zn, Mn and Fe, the concentration of Co was largely unchanged during the period of high NOM and trace metal flux, whilst marked depletions in V occurred antipathetically to spikes in Cu, Ni and Ti (Fig. 6a–e), possibly indicating dilution of NOM–V complexes in the dissolved fraction, i.e. V was not complexed by the coarse fraction (Tables 3 and 4), whereas some Co may have been carried by coarse colloids (Table 3), thereby compensating for reduced NOM–Co transport in finer fractions. In the following months the concentration of both Co and V slowly declined reaching a minimum between February and April 2009 after which their concentrations gradually increased (Fig. 6a–b). This decline was matched by a similar trend in the concentration of Ti, Ni and Cu in the fine and nominally dissolved size classes, although this trend was less pronounced than for Co and V (Fig. 6).

Both Co and V were concentrated in nominally dissolved size fraction (ca. 90% and 80%, respectively) with the remainder residing in the fine colloidal size range (Fig. 6a–b). Changes in the concentration of Co and V in both classes occurred synchronously, indicating that changes in the abundance of trace metal carriers in the fine and nominally dissolved size classes were controlled by similar processes. Most probably, this relates to the similar hydrodynamic properties of trace metal carriers in both the nominally dissolved and fine colloidal classes (i.e. with dimensions <100 nm). Importantly, the concentrations of Co and V were much higher in PE1 dripwater (Table 4) than in average HM rainfall



**Fig. 6.** Time series of trace metal concentrations in sequentially filtered PE1 dripwater samples collected between June 2008 and August 2009; (a) V (b) Co (c) Cu (d) Ti (e) Ni (f) Fe and Mn and (g) Zn; (h) weekly effective rainfall (P–E); and (i) daily rainfall. ND = nominally dissolved.

(Table 5), demonstrating inputs of NOM–metal complexes (Hartland et al., 2011) from the soil–aquifer system.

## 5. Discussion

### 5.1. High-flux and low-flux, NOM–metal transport in cave dripwaters

The accumulated data indicate that two prominent modes of NOM-facilitated trace metal transport occur in karst percolation waters: *high-flux* (high concentrations of coarse NOM and metals) and *low-flux* (low concentrations of fine and dissolved NOM and metals). In PE1 dripwater the first mode (high-flux) occurred in rapid, transient pulses in short order following peak infiltration events. Under high-flux conditions, Ti, Mn, Fe, Cu and Ni were mobilised by coarse colloids and particulates. Ratios of Cu:Ni between low- and high-flux events were distinctly different, indicating that binding to coarse (>100 nm) SOM by Cu and Ni occurs preferentially, probably because of a higher degree

of aromaticity when compared to small, humic-like colloids (Tipping, 2001). The second mode (low-flux) encompassed materials present in the fine colloidal and nominally dissolved size classes originating from rainwater and soils and was probably dominated by globular, humic- and fulvic-like colloids with diameters around 1–4 nm (Hartland et al., 2011). This is supported by the good agreement between measured Cu:Ni and Cu:Co at low-flux, Cu:Ni in HM rainwater and the predicted affinity ratios calculated from the equivalent  $n_1$  values for metal binding humic substances (Milne et al., 2003).

The low-flux mode was characterised by its own trace element signature, and variously included V, Co and Ti, typically concentrated in the nominally dissolved size class. However, a degree of crossover occurred and some Cu and Ni were also associated with this mode of transport. The extent to which each mode is important appears to vary between sites and drips, probably mediated by flow-routing. In LBG drip LB2–3 and PC drips BC1–2, large changes in trace metal partitioning between size classes were not detected. Despite substantial proportions of OC being detected in the particulate, coarse colloidal and fine colloidal size ranges, the surface-reactive metals Cu, Ni, and Co were uniformly concentrated in the nominally dissolved size range. Thus, because shifts in the ratio of these metals did not occur in these drips, changes in the size-distribution of NOM did not appear to coincide with a source change in NOM and may instead reflect aggregation processes, e.g. driven by carbonate dissolution (increasing ionic strength) and sufficiently long residence times.

In LBG drip LB1, ERN drips St-1 and St-2 and PC drip point PE1, Al, Ti, Fe, Ni, and Cu, as well as NOM (LB1 and PE1) revealed strong partitioning into the particulate size range during wetter periods. Experimental studies of the hydrodynamic behaviour of particles, colloids and solutes in fractured aquifer systems provide further insight into the results presented.

### 5.2. Hydrologic controls on NOM transmission

At Poole's Cavern, under slow, seepage-flow conditions in PE1 dripwater, fluorescent NOM in the fine and nominally dissolved size range showed an attenuated response to infiltration events. Rather than being transmitted in short pulses with particles, transmission of fine and nominally dissolved NOM was stretched out across several months. But, under fracture-fed flow conditions, we may reasonably suppose that fine organic colloids and DOM are transmitted much more rapidly.

These rationalisations fit within our understanding of the behaviour of artificial colloidal tracers in karstic aquifers under various flow conditions. Most studies have employed large latex microspheres with diameters between 1 and 5  $\mu\text{m}$  as surrogates for colloids (e.g. McKay et al., 1993; 2000). These studies show that under low-flow (i.e. low discharge) conditions, the breakthrough times of particles are faster than solutes ( $\text{Cl}^-$ , fluorescent dyes), but at high-flow this difference becomes less pronounced (McCarthy and Shevenell, 1998; Goppert and Goldscheider, 2008). Solutes are considered to migrate more slowly than small particles and coarse colloids at low-flow because of their tendency to diffuse into pore spaces and micro-fractures (McCarthy and McKay, 2004). Therefore, the results of this study indicate that at low-flow, fulvic- and humic-like colloids with diameters between ca. 1 and 4 nm (Hartland et al., 2011) probably behave similarly to dissolved tracers (e.g. Rhodamine, which has a similar molar mass (ca. 500) to the smallest humic components). It should be noted that the molar masses of humic-like compounds are not necessarily meaningful given that analytical methods are not directly comparable and give different answers (Sutton and Sposito, 2005; Lead and Wilkinson, 2006).

Unlike artificial tracers (which are not present in the aquifer prior to the experiment), natural organic colloids and dissolved NOM are probably already present in elevated concentrations within the diffuse permeability, and this sink for NOM may also prove to be a source providing a proportion of the net NOM export from the karst

aquifer. However, the results of monitoring of the PE1 dripwater, in particular the increased proportions of colloidal metals discharged in delayed response to peak infiltration events, suggest that some direct transmission of fine colloids from the soil, epikarst or directly contributed from infiltrating rainfall (Nimmo and Fones, 1997; Seitzinger et al., 2003; Muller et al., 2008) also occurred.

This has important implications for our understanding of the behaviour of NOM in karst and sheds new light on the results of previous studies which show that increases in dissolved organic carbon (DOC) concentration and fluorescence in cave dripwaters are often offset from rainfall events by several months (Baker et al., 1997, 2000; Cruz et al., 2005). Indeed, variations in fluorescence and DOC often are not related to variations in rainfall (Cruz et al., 2005), and where correlations occur, they improve at elevated discharge (Baker et al., 1997; Cruz et al., 2005) and in the most responsive drips (Ban et al., 2008).

From a survey of the literature it is evident that previous studies of NOM in cave dripwaters have focused on OC concentration below 0.45  $\mu\text{m}$  (i.e., “dissolved organic carbon” (DOC)) and fluorescence (e.g. Baker et al., 1997; Ban et al., 2008). However, because of the role of coarse colloids and particles in disruption of fluorescence signals it is not possible to determine whether fluorescence in these studies was disrupted by coarse colloids and particles (Hartland et al., 2010b). Furthermore, because all materials with a dimension  $>0.45 \mu\text{m}$  were traditionally removed, we cannot assess whether coarse colloidal/particulate NOM ( $> \text{ca. } 100 \text{ nm}$ ) and fine/nominally-dissolved fluorescent NOM ( $< \text{ca. } 100 \text{ nm}$ ) decoupled as a result of the divergent hydrodynamic properties of each component.

### 5.3. Controls on colloid and particle release from soils

Divergence in hydrological behaviour and the timing of breakthrough in dripwaters between particles and small colloids can be understood in terms of their hydrodynamic properties in fractured-rock aquifers. However, the processes affecting the release of these components from soils may also be important (e.g. for understanding speleothems). Colloids and particles are affected by changes in both solution chemistry and flow (Shevenell and McCarthy, 2002; Sen and Khilar, 2006), but because the distance of separation between fine colloids and pore surfaces may be very small ( $\sim 10^{-1} \text{ nm}$ ), van der Waals (short range) forces act more strongly on fine colloids (Rousseau et al., 2004).

Physiochemical processes at the interface between soil and aquifer solids and bulk solution are therefore central to understanding colloid retention and release. Small colloids including humic-like NOM and iron and manganese oxides, bind to soil and aquifer solids, forming films (Hering, 1995; Mayer and Xing, 2001); humic substances also form films on mineral colloids (Gibson et al., 2007) such as iron oxides, enhancing their surface charge and enabling their disaggregation and dispersion in solution (Baalousha, 2009).

The surface charge of fine colloids and nanoparticles, and whether they have a surface NOM film, are important controls on their release from surface sites and dispersion into solution. Release is favoured when the energy barrier on detachment is overcome by an increase in the charge of colloid and particle surfaces caused by a change in solution chemistry (Sen and Khilar, 2006) such as a change in the pH or reduction in the ionic strength of solution (Rousseau et al., 2004).

Larger particles are more strongly affected by hydrodynamic factors (Kaplan et al., 1993; Shevenell and McCarthy, 2002), but it is generally accepted that under flow rates typical of most natural systems (including karstic springs) hydrodynamic forces are less important than electrostatic adhesive/repulsive forces (Atteia et al., 1998; Sen and Khilar, 2006). Indeed, mobilisation of small colloids and decreases in pH appear to be correlated (Atteia and Kozel, 1997; Atteia et al., 1998). Thus, changes in soil pH, mediated by biogenic

$\text{CO}_2$  production, may lead to enhanced mobilisation of colloids from soils in summer and there is evidence indicating that dripwater DOC and reducing conditions in soils are correlated, allowing for temporal offsets (Cruz et al., 2005).

In addition to these factors, it has been shown that colloid release is also affected by initial soil moisture content (Rousseau et al., 2004) and the extent of delays between infiltration events (Schelde et al., 2002). Particle and colloid release is greatest during initial irrigation (El-Farhan et al., 2000), but may be enhanced by delays, allowing replenishment of the colloidal pool in soil water by diffusion (Schelde et al., 2002). This provides appropriate context for the PE1 dripwater results, which showed peak NOM mobilised during the first effective rainfall of early summer, and particle-associated trace metals being transmitted in discrete pulses, possibly reflecting the depletion and replenishment of colloids and particles in soil water by wetting and drying processes.

NOM mobilised from soils at peak infiltration may correlate with rainfall intensity, and this has been observed in cave waters in monsoonal regions where infiltration exceeds  $50 \text{ mm d}^{-1}$  (Ban et al., 2008). However, despite numerous column studies, the relation between colloid/particle mobilisation and flow remains ambiguous (Sen and Khilar, 2006). What is clear is that most mobilisation occurs during the upward and downward limbs of the infiltration hydrograph rather than at peak flow (El-Farhan et al., 2000; Cheng and Saiers, 2010), and larger particles experience the greatest hydrodynamic drag (Sen and Khilar, 2006). Thus, variations in metals in speleothems that are transported by soil-derived particles and coarse NOM (e.g. Fe, Y,  $\text{REE}^{3+}$ , Pb) may be more likely to correlate with infiltration intensity than metals transported by fine/nominally dissolved NOM.

### 5.4. Implications for the study of trace elements in speleothems

Evidence from speleothems points to NOM-mediated transport of transition metals, e.g. Y, Pb, Zn, Cu (Borsato et al., 2007); Pb and Zn (Fairchild et al., 2010); and Pb (Jo et al., 2010). For example, stalagmite ER78 from Grotta di Ernesto (corresponding to drip St-ER78) is characterised by annual fluorescent laminae which coincide with enrichments in a suite of elements including Y, Cu, Zn and Pb (Borsato et al., 2007). Of these elements, Y was most concentrated in the fluorescence zone, rapidly declining in concentration in the zone of growth corresponding to  $\pm 2$  months (Borsato et al., 2007). In the soil samples studied here, Y was distinguished from the other metals because it was present exclusively in the coarse fraction. However, the pattern of Y enrichment in ER78 is similar to that of Cu and Zn, possibly reflecting the fact that effective rainfall at ERN is limited to the autumn and winter (Borsato et al., 2007) and the significant hydrological differences between sites, e.g. greater proportions of fracture-fed flow (ERN) vs. more matrix-flow (PC).

Variations of trace elements that show specific affinities for high-flux or low-flux transport in cave dripwaters may be captured in speleothems and thus may provide information on the timing and magnitude of rainfalls. This is particularly relevant in regions with large extremes in seasonally effective rainfall where particulate NOM and associated metals (e.g. Fe, Y, Th,  $\text{REE}^{3+}$ , Pb) may potentially be mobilised by the kinetic energy of flow. For example, Jo et al. (2010) demonstrated a strong correlation between  $^{210}\text{Pb}_{\text{ex}}$  (excess, or unsupported  $^{210}\text{Pb}$ , i.e. that not derived from the radioactive decay series of  $^{238}\text{U}$ ) in a modern stalactite from Korea and rainfall amount in a region where summer typhoons dominate the annual rainfall distribution. Thus, under suitable conditions the mobilisation and transmission of metals associated with coarse NOM may occur in proportion to the magnitude of infiltration events. Alternatively, the correlation found by Jo et al. (2010) may simply reflect the efficiency of atmospheric scavenging of metals during cloud formation, and this topic should be addressed in future studies.

The speciation of specific organic constituents in cave dripwaters is yet to be examined in detail, but it is expected that lipids, DNA, spores, pollen and other materials are mobilised and transmitted in cave dripwaters during high NOM flux. Hence, changes in the ratio of metals (which directly compete for binding sites in NOM, e.g. Cu:Ni) in speleothems may indicate qualitative shifts in NOM composition, potentially aiding in the targeting of compound-specific, and other investigations of the organic fraction of speleothems (Blyth et al., 2008). Given that the low-flux (humic-like) trace metal signature probably corresponds to a mixture of sources (e.g. rainwater, soil water, diffuse permeability in aquifers) and shows temporal lags relative to infiltration, the high-flux metal signature in speleothems may offer the less ambiguous measure of infiltration and SOM composition.

NOM-facilitated trace metal transport may be of central importance for the incorporation of 'initial' Th in speleothems (Whitehead et al., 1999; Richter et al., 2004). Because trace metals display specific binding affinities for NOM in a range of sizes, resulting in a competitive hierarchy of trace element binding, it is reasonable to speculate that a range of other metals including Th may partition in a predictable manner, possibly enabling quantification of the excess 'detrital' Th in speleothems. Thus, this study of colloid-facilitated trace metal transport points to a potential new dimension in speleothem-based palaeoenvironmental analysis.

## 6. Conclusions

This study demonstrated for the first time that colloid- and particle-facilitated transport of trace metals occurs commonly in speleothem-forming groundwaters. Competitive binding of heavy metals to NOM in cave waters leads to characteristic shifts in trace metal ratios. Particulate SOM probably contains a larger proportion of high-energy binding sites than small humic-like colloids and thus at high particulate SOM flux, shifts to higher Cu:Ni occur because of the stronger competitive binding of Cu compared to Ni. In contrast, during periods of low NOM flux, humic- and fulvic-like compounds appear to dominate trace metal binding in cave waters with little metal partitioning into coarse colloids and particulates, consistent with weaker trace metal binding by aggregates. Under slow-flow conditions the migration of small fluorescent (humic- or fulvic-like) colloids occurs much more slowly than for coarse colloids and particulates, possibly leading to the temporally offset capture of both high-, and low-flux metal transport in speleothems.

## Acknowledgements

Thanks to the Natural Environment Research Council (NERC) for a studentship to AH (NER/S/A/2007/14396). The authors gratefully acknowledge the support of the NERC Facility for Environmental Nanoscience Analysis and Characterisation, University of Birmingham and NERC grant NE/G004048/1. Thanks to Alan Walker (Manager, Poole's Cavern), John Gunn (assistance with site selection), Arthur Price (LGBM site selection and access), Anna de Momi (field and lab support), Yon Ju Nam (AFM analyses) and Renza Miorandi (ERN site access and field logistics) for their invaluable assistance in facilitating this research. Special thanks to Stephen Baker for ICP-MS analyses.

## Appendix A. Supplementary data

Supplementary data to this article can be found online at doi:10.1016/j.chemgeo.2012.01.032.

## References

Aitken, G.R., Hsu-Kim, H., Ryan, J.N., 2011. Influence of dissolved organic matter on the environmental fate of metals, nanoparticles, and colloids. *Environmental Science & Technology* 45, 3196–3201.

- Atteia, O., Kozel, R., 1997. Particle size distributions in waters from a karstic aquifer: from particles to colloids. *Journal of Hydrology* 201 (1–4), 102–119.
- Atteia, O., Perret, D., Adatte, T., Kozel, R., Rossi, P., 1998. Characterization of natural colloids from a river and spring in a karstic basin. *Environmental Geology* 34 (4), 257–269.
- Baalousha, M., 2009. Aggregation and disaggregation of iron oxide nanoparticles: influence of particle concentration, pH and natural organic matter. *Science of the Total Environment* 407, 2093–2101.
- Baalousha, M., Lead, J.R., 2007. Characterization of natural aquatic colloids (<5 nm) by flow-field flow fractionation and atomic force microscopy. *Environmental Science & Technology* 41 (4), 1111–1117.
- Baker, A., Genty, D., 1999. Fluorescence wavelength and intensity variations of cave waters. *Journal of Hydrology* 217 (1–2), 19–34.
- Baker, A., Barnes, W.L., Smart, P.L., 1997. Variations in the discharge and organic matter content of stalagmite drip waters in Lower Cave, Bristol. *Hydrological Processes* 11 (11), 1541–1555.
- Baker, A., Mockler, N.J., Barnes, W.L., 1999a. Fluorescence intensity variations of speleothem-forming groundwaters: implications for paleoclimate reconstruction. *Water Resources Research* 35 (2), 407–413.
- Baker, A., Proctor, C.J., Barnes, W.L., 1999b. Variations in stalagmite luminescence laminae structure at Poole's Cavern, England, AD 1910–1996: calibration of a palaeoprecipitation proxy. *The Holocene* 9 (6), 683–688.
- Baker, A., Genty, D., Fairchild, I.J., 2000. Hydrological characterisation of stalagmite dripwaters at Grotte de Villars, Dordogne, by the analysis of inorganic species and luminescent organic matter. *Hydrology and Earth System Sciences* 4 (3), 439–449.
- Baker, A., Tipping, E., Thacker, S.A., Gondar, D., 2008. Relating dissolved organic matter fluorescence and functional properties. *Chemosphere* 73 (11), 1765–1772.
- Baldini, J.U.L., McDermott, F., Baker, A., Baldini, L.M., Matthey, D.P., Railsback, L.B., 2005. Biomass effects on stalagmite growth and isotope ratios: a 20th century analogue from Wiltshire, England. *Earth and Planetary Science Letters* 240, 486–494.
- Ban, F.M., Pan, G.X., Zhu, J., Cai, B.G., Tan, M., 2008. Temporal and spatial variations in the discharge and dissolved organic carbon of drip waters in Beijing Shihua Cave, China. *Hydrological Processes* 22 (18), 3749–3758.
- Bekhit, H.M., El-Kordy, M.A., Hassan, A.E., 2009. Contaminant transport in groundwater in the presence of colloids and bacteria: Model development and verification. *Journal of Contaminant Hydrology* 108, 152–167.
- Blyth, A.J., Baker, A., Collins, M.J., Penkman, K.E.H., Gilmour, M.A., Moss, J.S., Genty, D., Drysdale, R.N., 2008. Molecular organic matter in speleothems and its potential as an environmental proxy. *Quaternary Science Reviews* 27 (9–10), 905–921.
- Borsato, A., 2010. Dripwater monitoring at Grotta di Ernesto (NE Italy): a contribution to the understanding of karst hydrology and the kinetics of carbonate dissolution. *Proceedings of the 6th Conference on Limestone Hydrology and Fissured Media, vol. 2: La Chaux de Fonds. International Union of Speleology, Switzerland*, pp. 57–60.
- Borsato, A., Frisia, S., Fairchild, I.J., Somogyi, A., Susini, J., 2007. Trace element distribution in annual stalagmite laminae mapped by micrometer-resolution X-ray fluorescence: implications for incorporation of environmentally significant species. *Geochimica Et Cosmochimica Acta* 71 (6), 1494–1512.
- Buffle, J., Wilkinson, K.J., Stoll, S., Filella, M., Zhang, J.W., 1998. A generalized description of aquatic colloidal interactions: the three-colloidal component approach. *Environmental Science & Technology* 32 (19), 2887–2899.
- Chen, G., Flury, M., Harsh, J.B., Lichtner, P.C., 2005. Colloid-facilitated transport of cesium in variably saturated Hanford sediments. *Environmental Science & Technology* 39 (10), 3435–3442.
- Cheng, T., Saiers, J.E., 2010. Colloid-facilitated transport of cesium in vadose-zone sediments: the importance of flow transients. *Environmental Science & Technology* 44 (19), 7443–7449.
- Companys, E., Puy, J., Galceran, J., 2007. Humic acid complexation to Zn and Cd determined with the new electroanalytical technique AGNES. *Environmental Chemistry* 4 (5), 347–354.
- Cruz, F.W., Karmann, I., Magdalenó, G.B., Coichev, N., Viana, O., 2005. Influence of hydrological and climatic parameters on spatial-temporal variability of fluorescence intensity and DOC of karst percolation waters in the Santana Cave System, Southeastern Brazil. *Journal of Hydrology* 302 (1–4), 1–12.
- Defra, 2012. Department for Food, Environment and Rural Affairs, Rural Heavy Metals Network. <http://uk-air.defra.gov.uk/networks/network-info?view=rm>. Accessed 20/1/2012.
- Doucet, F.J., Lead, J.R., Santschi, P.H., 2007. Colloid-trace element interactions in aquatic systems. In: Wilkinson, K., Lead, J. (Eds.), *Environmental Colloids and Particles: Behaviour, Separation and Characterisation*.
- Einsiedl, F., Hertkorn, N., Wolf, M., Frommberger, M., Schmitt-Kopplin, P., Koch, B.P., 2007. Rapid biotic molecular transformation of fulvic acids in a karst aquifer. *Geochimica et Cosmochimica Acta* 71, 5474–5482.
- El-Farhan, Y.H., Denovio, N.M., Herman, J.S., Hornberger, G.M., 2000. Mobilization and transport of soil particles during infiltration experiments in an agricultural field, Shenandoah Valley, Virginia. *Environmental Science & Technology* 34 (17), 3555–3559.
- Fairchild, I.J., Hartland, A., 2010. Trace element variations in stalagmites: controls by climate and by karst system processes. In: Stoll, H., Prieto, M. (Eds.), *Ion Partitioning in Ambient Temperature Aqueous Systems: From Fundamentals to Applications in Climate Proxies and Environmental Geochemistry*. EMU Notes in Mineralogy 10, European Mineralogical Union and the Mineralogical Society of Great Britain and Ireland, London, pp. 259–283.
- Fairchild, I.J., Treble, P.C., 2009. Trace elements in speleothems as recorders of environmental change. *Quaternary Science Reviews* 28 (5–6), 449–468.

- Fairchild, I.J., Borsato, A., Tooth, A.F., Frisia, S., Hawkesworth, C.J., Huang, Y.M., McDermott, F., Spiro, B., 2000. Controls on trace element (Sr-Mg) compositions of carbonate cave waters: implications for speleothem climatic records. *Chemical Geology* 166, 255–269.
- Fairchild, I.J., Smith, C.L., Baker, A., Fuller, L., Spotl, C., Matthey, D., McDermott, F., 2006a. Modification and preservation of environmental signals in speleothems. *Earth-Science Reviews* 75 (1–4), 105–153.
- Fairchild, I.J., Tuckwell, G.W., Baker, A., Tooth, A.F., 2006b. Modelling of dripwater hydrology and hydrogeochemistry in a weakly karstified aquifer (Bath, UK): implications for climate change studies. *Journal of Hydrology* 321 (1–4), 213–231.
- Fairchild, I.J., Loader, N.J., Wynn, P.M., Frisia, S., Thomas, P.A., Lageard, J.G.A., De Momi, A., Hartland, A., Borsato, A., La Porta, N., Susini, J., 2009. Sulfur fixation in wood mapped by synchrotron X-ray studies: implications for environmental archives. *Environmental Science & Technology* 43, 1310–1315.
- Fairchild, I.J., Spotl, C., Frisia, S., Borsato, A., Susini, J., Wynn, P.M., Caudiz, J., EIMF, 2010. Petrology and geochemistry of annually laminated stalagmites from an Alpine cave (Obir, Austria): seasonal cave physiology. *Geological Society, London, Special Publications* 336, 295–321.
- Filella, M., 2008. NOM site binding heterogeneity in natural waters: discrete approaches. *Journal of Molecular Liquids* 143, 42–51.
- Frisia, S., Borsato, A., Fairchild, I.J., McDermott, F., 2000. Calcite fabrics, growth mechanisms, and environments of formation in speleothems from the Italian Alps and southwestern Ireland. *Journal of Sedimentary Research* 70, 1183–1196.
- Frisia, S., Borsato, A., Spotl, C., Villa, I.M., Cucchi, F., 2005. Climate variability in the SE Alps of Italy over the past 17 000 years reconstructed from a stalagmite record. *Boreas* 34, 445–455.
- Gibson, C.T., Turner, I.J., Roberts, C.J., Lead, J.R., 2007. Quantifying the dimensions of nanoscale organic surface layers in natural waters. *Environmental Science & Technology* 41, 1339–1344.
- Gilfedder, B.S., Petri, M., Biester, H., 2007. Iodine and bromine speciation in snow and the effect of orographically induced precipitation. *Atmospheric Chemistry and Physics* 7, 2661–2669.
- Goppert, N., Goldscheider, N., 2008. Solute and colloid transport in karst conduits under low- and high-flow conditions. *Ground Water* 46 (1), 61–68.
- Groenenberg, J.E., Koopmans, G.F., Comans, R.N.J., 2010. Uncertainty analysis of the nonideal competitive adsorption-Donnan model: effects of dissolved organic matter variability on predicted metal speciation in soil solution. *Environmental Science & Technology* 44, 1340–1346.
- Hartland, A., Fairchild, I.J., Lead, J.R., Dominguez-Villar, D., Baker, A., Gunn, J., Baalousha, M., Ju-Nam, Y., 2010a. The dripwaters and speleothems of Poole's Cavern: a review of recent and ongoing research. *Cave and Karst Science* 36 (2), 37–46.
- Hartland, A., Fairchild, I.J., Lead, J.R., Baker, A., 2010b. Fluorescent properties of organic carbon in cave dripwaters: effects of filtration, temperature and pH. *Science of the Total Environment* 408 (23), 5940–5950.
- Hartland, A., Fairchild, I.J., Lead, J.R., Zhang, H., Baalousha, M., 2011. Size, speciation and lability of NOM-metal complexes in a hyperalkaline cave dripwater. *Geochemica et Cosmochimica Acta* 75, 7533–7551.
- Hering, J.G., 1995. Interaction of organic-matter with mineral surfaces – effects on geochemical processes at the mineral-water interface. *Aquatic Chemistry* 244, 95–110.
- Huang, H.M., Fairchild, I.J., Borsato, A., Frisia, S., Cassidy, N.J., McDermott, F., Hawkesworth, C.J., 2001. Seasonal variations in Sr, Mg and P in modern speleothems (Grotta di Ernesto, Italy). *Chemical Geology* 175, 429–448.
- Hudson, N., Baker, A., Reynolds, D., 2007. Fluorescence analysis of dissolved organic matter in natural, waste and polluted waters – a review. *River Research and Applications* 23 (6), 631–649.
- Jo, K.N., Woo, K.S., Hong, G.H., Kim, S.H., Suk, B.C., 2010. Rainfall and hydrological controls on speleothem geochemistry during climatic events (droughts and typhoons): an example from Seopdong Cave, Republic of Korea. *Earth and Planetary Science Letters* 295 (3–4), 441–450.
- Kaplan, D.L., Bertsch, P.M., Adriano, D.C., Miller, W.P., 1993. Soil-borne mobile colloids as influenced by water flow and organic carbon. *Environmental Science and Technology* 27 (6), 1193–1200.
- Kelleher, B.P., Simpson, A.J., 2006. Humic substances in soils: are they really chemically distinct? *Environmental Science & Technology* 40, 4605–4611.
- Kersting, A.B., Efund, D.W., Finnegan, D.L., Rokop, D.J., Smith, D.K., Thompson, J.L., 1999. Migration of plutonium in ground water at the Nevada Test Site. *Nature* 397 (6714), 56–59.
- Kinniburgh, D.G., van Riemsdijk, W.H., Koopal, L.K., Borkovec, M., Benedetti, M.F., Avena, M.J., 1999. Ion binding to natural organic matter: competition, heterogeneity, stoichiometry and thermodynamic consistency. *Colloids and Surfaces A—Physicochemical and Engineering Aspects* 151 (1–2), 147–166.
- Lead, J.R., Wilkinson, K.J., 2006. Aquatic colloids and nanoparticles: current knowledge and future trends. *Environmental Chemistry* 3 (3), 159–171.
- Lead, J.R., Davison, W., Hamilton-Taylor, J., Buffle, J., 1997. Characterising colloidal material in natural waters. *Analytical Geochemistry* 3, 213–232.
- Liu, R., Lead, J.R., 2006. Partial validation of cross flow ultrafiltration by atomic force microscopy. *Analytical Chemistry* 78, 8105–8112.
- Marang, L., Eidner, S., Kumke, M.U., Benedetti, M.F., Reiller, P.E., 2009. Spectroscopic characterization of the competitive binding of Eu(III), Ca(II), and Cu(II) to a sedimentary originated humic acid. *Chemical Geology* 264 (1–4), 154–161.
- Mavrocordatos, D., Mondy-Couture, C., Atteia, O., Leppard, G.G., Perret, D., 2000. Formation of a distinct class of Fe-Ca(-C-org)-rich particles in a complex peat-karst system. *Journal of Hydrology* 237 (3–4), 234–247.
- Mayer, L.M., Xing, B.S., 2001. Organic matter—surface area relationships in acid soils. *Soil Science Society of America Journal* 65, 250–258.
- McCarthy, J.F., McKay, L.D., 2004. Colloid transport in the subsurface: past, present, and future challenges. *Vadose Zone Journal* 3 (2), 326–337.
- McCarthy, J.F., Shevenell, L., 1998. Processes controlling colloid composition in a fractured and karstic aquifer in eastern Tennessee, USA. *Journal of Hydrology* 206 (3–4), 191–218.
- McKay, L.D., Gillham, R.W., Cherry, J.A., 1993. Field experiments in a fractured clay till. 2. Solute and colloid transport. *Water Resources Research* 29 (12), 3879–3890.
- McKay, L.D., Sanford, W.E., Strong, J.M., 2000. Field-scale migration of colloidal tracers in a fractured shale saprolite. *Ground Water* 38 (1), 139–147.
- Milne, C.J., Kinniburgh, D.G., Van Riemsdijk, W.H., Tipping, E., 2003. Generic NICA-Donnan model parameters for metal-ion binding by humic substances. *Environmental Science & Technology* 37, 958–971.
- Miorandi, R., Borsato, A., Frisia, S., Fairchild, I.J., Richter, D.K., 2010. Epikarst hydrology and implications for stalagmite capture of climate changes at Grotta di Ernesto (NE Italy): results from long-term monitoring. *Hydrological Processes* 24 (21), 3101–3114.
- Muller, C.L., Baker, A., Hutchinson, R., Fairchild, I.J., Kidd, C., 2008. Analysis of rainwater dissolved organic carbon compounds using fluorescence spectroscopy. *Atmospheric Environment* 42, 8036–8045.
- Nimmo, M., Fones, G.R., 1997. The potential pool of Co, Ni, Cu, Pb and Cd organic complexing ligands in coastal and urban rain waters. *Atmospheric Environment* 31, 693–702.
- NSRI, 2008. Soils Site Report, National Grid Reference ST8790099194; Area 1 km × 1 km. National Soil Resources Institute, Cranfield University. Accessed via <https://www.landis.org.uk/sitereporter/>.
- Pedrot, M., Dia, A., Davranche, M., Bouhnik-Le Coz, M., Henin, O., Gruau, G., 2008. Insights into colloid-mediated trace element release at the soil/water interface. *Journal of Colloid and Interface Science* 325 (1), 187–197.
- Richter, D.K., Gotte, T., Niggemann, S., Wurth, G., 2004. REE<sup>3+</sup> and Mn<sup>2+</sup> activated cathodoluminescence in late glacial and Holocene stalagmites of central Europe: evidence for climatic processes? *The Holocene* 14 (5), 759–767.
- Roberts, M.S., Smart, P.L., Baker, A., 1998. Annual trace element variations in a Holocene speleothem. *Earth and Planetary Science Letters* 154, 237–246.
- Rousseau, M., Di Pietro, L., Angulo-Jaramillo, R., Tessier, D., Cabibel, B., 2004. Preferential transport of soil colloidal particles: physicochemical effects on particle mobilization. *Vadose Zone Journal* 3 (1), 247–261.
- Schelde, K., Moldrup, P., Jacobsen, O.H., de Jonge, H., de Jonge, L.W., Komatsu, T., 2002. Diffusion-limited mobilization and transport of natural colloids in macroporous soil. *Vadose Zone Journal* 1 (1), 125–136.
- Seitzinger, S.P., Styles, R.M., Lauck, R., Mazurek, M.A., 2003. Atmospheric pressure mass spectrometry: a new analytical chemical characterization method for dissolved organic matter in rainwater. *Environmental Science & Technology* 37, 131–137.
- Sen, T.K., Khilar, K.C., 2006. Review on subsurface colloids and colloid-associated contaminant transport in saturated porous media. *Advances in Colloid and Interface Science* 119 (2–3), 71–96.
- Senesi, N., Miano, T.M., Provenzano, M.R., Brunetti, G., 1991. Characterization, differentiation, and classification of humic substances by fluorescence spectroscopy. *Soil Science* 152 (4), 259–271.
- Shaw, E.M., 1994. *Hydrology in Practice*. Routledge, Abingdon.
- Shevenell, L., McCarthy, J.F., 2002. Effects of precipitation events on colloids in a karst aquifer. *Journal of Hydrology* 255 (1–4), 50–68.
- Smart, P.L., Friedrich, H., 1987. 'Water movement and storage in the unsaturated zone of a maturely karstified aquifer, Mendip Hills, England', Proceedings, Conference on Environmental Problems in Karst Terrains and Their Solution, Bowling Green, Kentucky. National Water Well Association, pp. 57–87.
- Sumbler, M.G., Barron, A.J.M., Morigi, A.N., 2000. *Geology of the Cirencester district. Memoir of the British Geological Survey*.
- Sutton, R., Sposito, G., 2005. Molecular structure in humic substances: the new view. *Environmental Science & Technology* 39, 9009–9015.
- Tan, M., Baker, A., Genty, D., Smith, C., Esper, J., Cai, B.G., 2006. Applications of stalagmite laminae to paleoclimate reconstructions: comparison with dendrochronology/climatology. *Quaternary Science Reviews* 25 (17–18), 2103–2117.
- Tipping, E., 1998. Humic ion-binding model VI: an improved description of the interactions of protons and metal ions with humic substances. *Aquatic Geochemistry* 4, 3–48.
- Tipping, E., 2001. *Cation Binding by Humic Substances*. University Press, Cambridge.
- Tooth, A.F., Fairchild, I.J., 2003. Soil and karst aquifer hydrological controls on the geochemical evolution of speleothem-forming drip waters, Crag Cave, southwest Ireland. *Journal of Hydrology* 273 (1–4), 51–68.
- Unsworth, E.R., Warnken, K.W., Zhang, H., Davison, W., Black, F., Buffle, J., Cao, J., Clevin, R., Galceran, J., Gunkel, P., Kalis, E., Kistler, D., Van Leeuwen, H.P., Martin, M., Noel, S., Nur, Y., Odzak, N., Puy, J., Van Riemsdijk, W., Sigg, L., Temminghoff, E., Tercier-Waeber, M.L., Toepferwien, S., Town, R.M., Weng, L.P., Xue, H.B., et al., 2006. Model predictions of metal speciation in freshwaters compared to measurements by in situ techniques. *Environmental Science & Technology* 40, 1942–1949.
- Verdugo, P., Orellana, M.V., Chin, W.C., Petersen, T.W., van den Eng, G., Benner, R., Hedges, J.L., 2008. Marine biopolymer self-assembly: implications for carbon cycling in the ocean. *Faraday Discussions* 139, 393–398.
- Warnken, K.W., Davison, W., Zhang, H., Galceran, J., Puy, J., 2007. In situ measurements of metal complex exchange kinetics in freshwater. *Environmental Science & Technology* 41 (9), 3179–3185.
- White, H.K., Xu, L., Lima, A.L.C., Eglinton, T.I., Reddy, C.M., 2005. Abundance, composition, and vertical transport of PAHs in marsh sediments. *Environmental Science & Technology* 39 (21), 8273–8280.
- Whitehead, N.E., Ditchburn, R.G., Williams, P.W., McCabe, W.J., 1999. Pa-231 and Th-230 contamination at zero age: a possible limitation on U/Th series dating of speleothem material. *Chemical Geology* 156 (1–4), 359–366.
- Witt, M., Jickells, T., 2005. Copper complexation in marine and terrestrial rain water. *Atmospheric Environment* 39, 7657–7666.
- Zhou, H., Wang, Q., Zhao, J., Zheng, L., Guan, H., Feng, Y., Greig, A., 2008. Rare earth elements and yttrium in a stalagmite from Central China and potential paleoclimatic implications. *Palaeogeography Palaeoclimatology Palaeoecology* 270, 128–138.